AD-A155 524 THE EFFECTS OF SUBREFRACTIVE LAYERS AND ELEVATED DUCTS 1/1
ON AIRBORNE RADAR AND ESM (ELECTRONIC SURVEILLANCE
MEASURES)(U) NAVAL POSTGRADUATE SCHOOL MONTEREY CA
UNCLASSIFIED D D GRAU MAR 85 F/G 17/9 NL

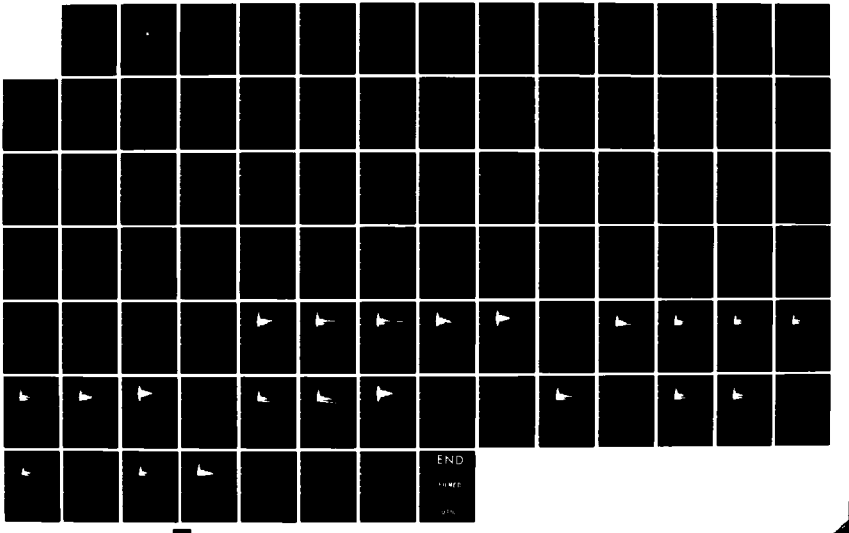

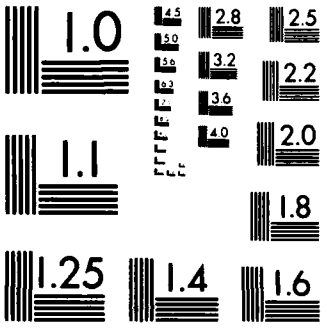

MICROCOPY RESOLUTION TEST CHART
NATIONAL BUREAU OF STANDARDS-1963-A

(2)

NAVAL POSTGRADUATE SCHOOL
Monterey, California

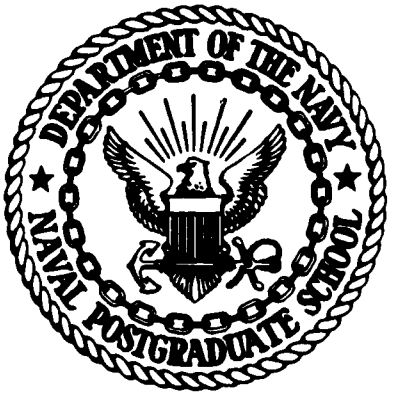

THESIS

THE EFFECTS OF SUBREFRACTIVE LAYERS AND ELEVATED DUCTS ON AIRBORNE RADAR AND ESM

by

Douglas D. Grau

March 1985

Thesis Advisor: William J. Shaw

Approved for public release; distribution is unlimited.

SECURITY CLASSIFICATION OF THIS PAGE *(When Data Entered)*

REPORT DOCUMENTATION PAGE		READ INSTRUCTIONS BEFORE COMPLETING FORM
1. REPORT NUMBER	2. GOVT ACCESSION NO.	3. RECIPIENT'S CATALOG NUMBER
4. TITLE *(and Subtitle)* The Effects of Subrefractive Layers and Elevated Ducts on Airborne Radar and ESM		5. TYPE OF REPORT & PERIOD COVERED Master's Thesis March, 1985 6. PERFORMING ORG. REPORT NUMBER
7. AUTHOR(s) Douglas D. Grau		8. CONTRACT OR GRANT NUMBER(s)
9. PERFORMING ORGANIZATION NAME AND ADDRESS Naval Postgraduate School Monterey, CA 93943		10. PROGRAM ELEMENT, PROJECT, TASK AREA & WORK UNIT NUMBERS
11. CONTROLLING OFFICE NAME AND ADDRESS Naval Postgraduate School Monterey, CA 93943		12. REPORT DATE March, 1985 13. NUMBER OF PAGES 89
14. MONITORING AGENCY NAME & ADDRESS*(if different from Controlling Office)*		15. SECURITY CLASS. *(of this report)* 15a. DECLASSIFICATION/DOWNGRADING SCHEDULE

16. DISTRIBUTION STATEMENT *(of this Report)*

Approved for public release; distribution is unlimited.

17. DISTRIBUTION STATEMENT *(of the abstract entered in Block 20, if different from Report)*

18. SUPPLEMENTARY NOTES

19. KEY WORDS *(Continue on reverse side if necessary and identify by block number)*

anomalous propagation, subrefractive layers, ducting

20. ABSTRACT *(Continue on reverse side if necessary and identify by block number)*

This report is an investigation of the effects of anomalous propagation of radar waves, caused by subrefractive layers and elevated ducts, on aircraft radar performance and possible tactics. A test and evaluation of radar coverage for various environmental scenarios is conducted using the Integrated Refractive Effects Prediction System (IREPS) model. From the results of each scenario, a decision matrix is created and

DD FORM 1 JAN 73 1473 EDITION OF 1 NOV 65 IS OBSOLETE

S/N 0102-LF-014-6601

SECURITY CLASSIFICATION OF THIS PAGE *(When Data Entered)*

20. ABSTRACT

applied as an analysis tool for determining satisfactory flight profiles for a given mission. The findings are discussed from both a radiating and non-radiating aircraft perspective. Environmental data collected from the Mediterranean Sea and Northern Arabian Sea were analyzed and used to determine the test scenarios.

Approved for public release; distribution is unlimited.

The Effects of Subrefractive Layers and Elevated Ducts on Airborne Radar and ESM

by

Douglas D. Grau
Lieutenant, United States Navy
B.S., United States Naval Academy, 1978

Submitted in partial fulfillment of the
requirements for the degree of

MASTER OF SCIENCE IN OPERATIONS RESEARCH

from the

NAVAL POSTGRADUATE SCHOOL
March 1985

Author: Douglas D. Grau
Douglas D. Grau

Approved by: W.J. Shaw
W.J. Shaw, Thesis Advisor

T.H. Bolvik, Second Reader

A.R. Washburn, Chairman,
Department of Operations Research

Kneale T. Marshall
Kneale T. Marshall,
Dean of Information and Policy Sciences

ABSTRACT

This report is an investigation of the effects of anomalous propagation of radar waves, caused by subrefractive layers and elevated ducts, on aircraft radar performance and possible tactics. A test and evaluation of radar coverage for various environmental scenarios is conducted using the Integrated Refractive Effects Prediction System (IREPS) model. From the results of each scenario, a decision matrix is created and applied as an analysis tool for determining satisfactory flight profiles for a given mission. The findings are discussed from both a radiating and a non-radiating aircraft perspective. Environmental data collected from the Mediterranean Sea and Northern Arabian Sea were analyzed and used to determine the test scenarios.

TABLE OF CONTENTS

I. INTRODUCTION

Naval aviation operations involving airborne early warning (AEW) and reconnaissance aircraft are continually striving to increase the probability of successfully detecting hostile aircraft. In order for the search aircraft to optimize its efforts, it must take advantage of all phases of the detection process. An understanding of the effects of anomalous propagation of radar waves through the environment is one area of the search and detection scenario that may contribute toward improving the probability of detection. If this knowledge is properly exploited, a tactical advantage over an adversary may be gained.

The purpose of this study is to investigate the performance and tactical effects that anomalous atmospheric refraction conditions may have on airborne radars and electronic surveillance measures (ESM) in AEW and reconnaissance aircraft. The operations research involved with AEW and ESM aircraft in the atmosphere is complicated by the existance of refractive layers which alter normal radar propagation. The methods used for analysis of this problem were tests and evaluations of controlled simulations on the Integrated Refractive Effects Prediction System (IREPS) model [Ref. 1]. A wide variety of environmental profiles were applied to the IREPS model, which was developed by the Naval Ocean Systems Center (NOSC) of San Diego, Ca. The intention was to determine the possible tactical placement of an aircraft (AEW/ESM) relative to selected subrefractive layers and elevated ducts of varying strengths and thicknesses. By creating several test scenarios involving these atmospheric conditions and positioning a radar source at various altitudes with respect

to the layers, a better insight into the problem was achieved. The IREPS program was used to help predict the location of possible radar fading or areas of diminished probability of detection for each scenario. The IREPS program is operated on an HP 9845 desk-top computer and uses ray tracing of radar waves and a graphical display to convey the results. The IREPS graphical representations were analyzed to estimate the optimal flight altitude for a given subrefractive or elevated trapping layer. Once the information about each test scenario was collected and a quantitative analysis performed on the data, a decision matrix was constructed to further assist in predicting potential flight profiles for an AEW or reconnaissance aircraft. This type of tactical analysis, based upon environmental scenarios, is supported by an analysis of refraction climatology.

Radiosonde data which were collected in the Eastern Mediterranean Sea and Northern Arabian Sea by United States aircraft carriers provided information used in an environmental analysis of these areas. Using both APL and a graphical statistics package (Grafstat) on the IBM 3033, a data analysis consisting of the frequency of occurrence, the altitude profile, and the physical structure of the anomalous layers was obtained. The data collected were further used to substantiate the selected test profiles.

II. BACKGROUND

This study is concerned with the lower part of the atmosphere known as the troposphere which ranges from sea level to approximately 30,000 to 60,000 ft. The troposphere is a variable region of the atmosphere in which temperature, humidity and pressure generally decrease with an increase in altitude. This type of environment affects the propagation of electromagnetic (EM) waves in several ways: reflections, refractions and attenuation [Ref. 2 p. 1]. Refraction, or bending of EM waves, will be the primary topic of this study.

Refraction of radio waves is due to changes of the refractive index with altitude. The refractive index (n) for a medium is defined as the ratio of velocity of propagation of the electromagnetic (EM) wave in a vacuum to the velocity of propagation of the EM wave in that medium. Electromagnetic waves travel faster in a vacuum than in air, therefore yielding a refractive index (n) slighty greater than one [Ref. 3 p. 75]. The average value for the refractive index is 1.00035, measured at sea level. Often for numerical convenience, refractivity N is substituted for the refractive index n.

$$N = (n-1)\times 10^6 \qquad (2.1)$$

The refractivity (N) is dependent upon pressure P(mbar), temperature T(deg K) and water vapor pressure e(mbar). The relationship is as fcllows:

$$N = 77.6(P/T) + 3.73\times 10^5\ (e/T^2) \qquad (2.2)$$

This equation is valid within 0.5% for the following variable tolerances: atmospheric pressures between 200 mb

and 1100 mb, air temperatures (T) between 240 and 310 degrees k, water vapor pressures (e) less than 30 mb, and radio frequencies (f) less than 30 GHz [Ref. 2 p. 14]. Under ordinary atmospheric conditions, surface refractivity (N) ranges from 240 to 400 N units [Ref. 3 p. 75]. Often, for convenience, a modified refractivity M is substituted for refractivity N. M is defined so that when dM/dh is negative, trapping layers exist. The relationship between M and N is shown by equation 2.3.

$$M = N + (h/a)x10^6 \qquad (2.3)$$

The variable h is altitude and a is the earth's radius [Ref. 2 p. 27].

Variations of meteorological conditions cause variations in the refractivity N through fluctuations in the temperature, water vapor pressure and atmospheric pressure. When the refractivity gradient is equal to -48 N units/kft (-157 N units/km), the electromagnetic rays will be bent to follow the curvature of the earth. If this or a more negative gradient exists and is horizontally uniform (homogeneous) in the atmosphere, a duct is formed. The trapping of radio waves in the duct is primarily dependent upon the strength of the gradient (dN/dh) and the thickness of the duct [Ref. 4]. Given a duct thickness, the ability to trap the radio waves is related to the EM frequency. The part of the electromagnetic spectrum that can be trapped in the troposphere consists of frequencies greater than 100 MHz.

One important characteristic of a duct with respect to radar propagation is the minimum thickness required for trapping [Ref. 5]. Table 1 represents the relationship between the frequency of a radio wave and the minimum duct thickness required to trap the wave. HF frequencies are not typically trapped because of the thickness necessary for trapping to occur [Ref. 6].

TABLE 1

Relationship of Frequency to Minimum Duct Thickness Required for Trapping

frequency band (MHz)		wavelength (cm)	min. duct thickness (ft)	min. duct thickness (m)
0		0		
50	A	600	2,054.8	626.3
250		120	410.8	125.2
	B			
500		60	205.4	62.6
	C			
1,000		30	102.7	31.3
	D			
2,000		15	51.5	15.7
	E			
3,000		10	34.1	10.4
	F			
4,000		7.5	25.6	7.8
	G			
6,000		5	17.1	5.2
	H			
8,000		3.75	12.8	3.9
	I			
10,000		3	10.2	3.1
	J			
20,000		1.5	5.2	1.6
	K			
40,000		.75	2.6	0.8
	L			
60,000		.5	1.6	0.5
	M			
100,000		.3	1.3	0.4
450*		67	228.3	69.6

$$D = 7.86 \times 10^4 / (f\sqrt{\Delta M})$$

D = thickness of duct (meters)

ΔM = change in modified refractivity across the trapping layer

(for the test example $\Delta M = 6.3$)

f = frequency (MHz)

* frequency of test radar

Anomalous refraction causing trapping and ducting of EM waves within strong refracting layers in the atmosphere may cause extended ranges for radar coverage. This increase in EM energy within refractive layers must result in a decrease of EM energy above these trapping layers. The regions of decreased EM energy are referred to as radar holes or areas of radar fading. Because energy leakage out of the ducts may exist, the radar holes are not completely void of coverage but rather are areas of diminished probability of detection as a result of signal attenuation [Ref. 7]. Surface reflections of radar waves off the earth will also contribute towards radar coverage.

If the refractivity gradient (dN/dh) is positive, EM waves will bend away from the earth. This results in the formation of a subrefractive layer. Figure 2.1 illustrates the direction of wave bending for various refraction conditions. Any bending of radar waves other than standard refraction of EM rays (which occurs in an averaged atmosphere) is referred to as anomalous refraction. The development of both subrefractive layers and elevated trapping layers will be discussed later in the text.

The data used to calculate the refractive gradient are collected by means of radiosondes, dropsondes and airborne microwave refractometers (AMR). These instruments sample the atmosphere at various altitudes and record the temperature, pressure, and humidity in the case of radiosondes and dropsondes, while the actual index of refraction is computed by the refractometer. The radiosonde data for the Navy are collected by weather balloons that are launched from the ships.

Several inherent operational problems are encountered when the sampling is conducted in this manner. The launching opportunity of the balloon is frequently

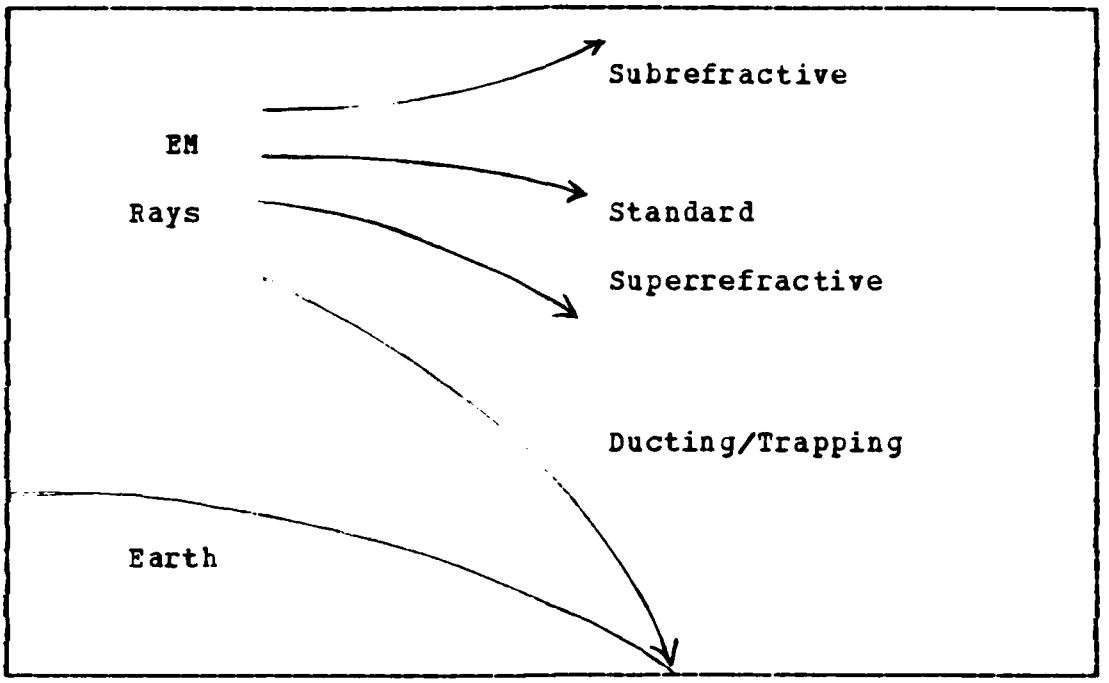

Figure 2.1 Categories of Anomalous Wave Propagation

determined by flight operations, especially aboard the carriers. The information that is collected by the balloon is only accurate for the immediate vicinity of the launching ship. However, the information is applied to a larger area by assuming a homogeneous atmosphere. This assumption often applies over the ocean, but it is not valid near the coast. When an airborne microwave refractometer is used by the aircraft, a sampling of the atmosphere can be taken in the immediate patrolling area, thus providing the actual information on a real time basis.

A. METHODOLOGY

This study consists of tests and evaluations of the effects of various predetermined environmental profiles on radar wave propagation. The environmental scenarios of

interest included a subrefractive layer, an elevated duct, and combinations of both a subrefractive layer and an elevated duct. Once each test scenario was created, simulation trials were then conducted using IREPS by positioning a radar source below, in, and above the refractive layers. The purpose of these trials was to determine what possible effects the anomalies may have on the radar wave propagation. From the information provided through the IREPS model, several measures of effectiveness (MOE) were developed. The following are the measures of effectiveness that were utilized in the analysis of each radar coverage:

1. Distance of the aircraft's radar horizon (nm).

The airborne early warning (AEW) aircraft can increase its potential radar coverage area by maximizing the distance to its radar horizon subject to the aircraft's flight limitations. This MOE is based upon a standard atmosphere computation.

2. Distance from aircraft to area of radar distortion (nm).

The radiating aircraft can improve its radar coverage by keeping the distance to the area of radar distortion at the maximum possible range.

3. Approximate cross-sectional area in the vertical plane of radar distortion (nm^2).

To provide the best possible coverage, the radiating aircraft should minimize the cross-sectional area of radar distortion. A radar range of 200 nm was used for this calculation.

These measures of effectiveness are demonstrated in Figure 2.2 [Ref. 8].

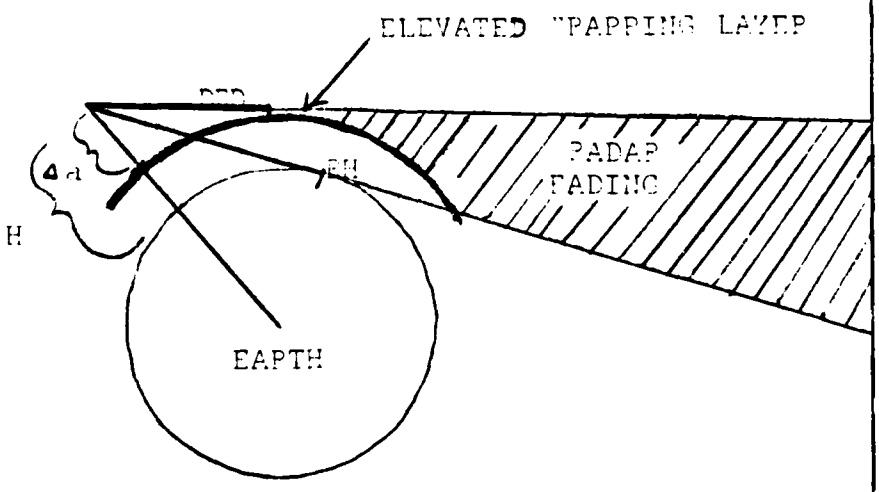

RH (radar horizon (nm)) = $Kc\sqrt{H}$

DRD (distance to radar distortion (nm)) = $Kc\sqrt{\Delta a}$

Kc = 1.23 effective earth radius conversion constant

Kc is the effective earth radius conversion constant taken from 4/3 earth radius calculation.

H = altitude of radar source (ft)

Δa = change in height above layer (ft)

Figure 2.2 Radar Horizon and MOE Diagram

Once the results of the refractive layers were calculated, a decision matrix was developed to assist the decision maker in tactical flight planning. The matrix was constructed using the possible future states of nature that an AEW aircraft could experience and the alternative decisions about flight altitudes associated with the future states. The altitudes of the refractive layers (i.e. subrefractive layer or elevated duct) were considered the future states of nature. These states were assumed to be mutually exclusive and collectively exhaustive. The states of nature are represented in the decision matrix by the set S1,...Sj and the alternatives are represented by the set A1,...Ai. The decision matrix also consists of payoff values for each type of decision. The payoffs are represented by Vij [Ref. 9]. The payoff values for the actual test examples are the relative values of the defined radar coverage according to the measures of effectiveness. The measures of effectiveness were used in a two step process. First, the cross-sectional area of the radar distortion and the distance to the radar distortion were used to establish the matrix payoffs and then the aircraft's radar horizon is used by the decision maker to choose between alternatives of equal payoff value. A sample of the decision matrix format is shown in Figure 2.3 .

For the decision matrix used in the test examples, the probabilities of each state occurring, Pj, will be known. This is attributed to environmental information about the location of the refractive layers gained through the use of an airborne microwave refractometer or radiosondes. Once the decision matrix for each example has been constructed, the information is transformed to a graphical aid representing refractive layers and flight altitudes. Each environmental test scenario will undergo a similar type of analysis.

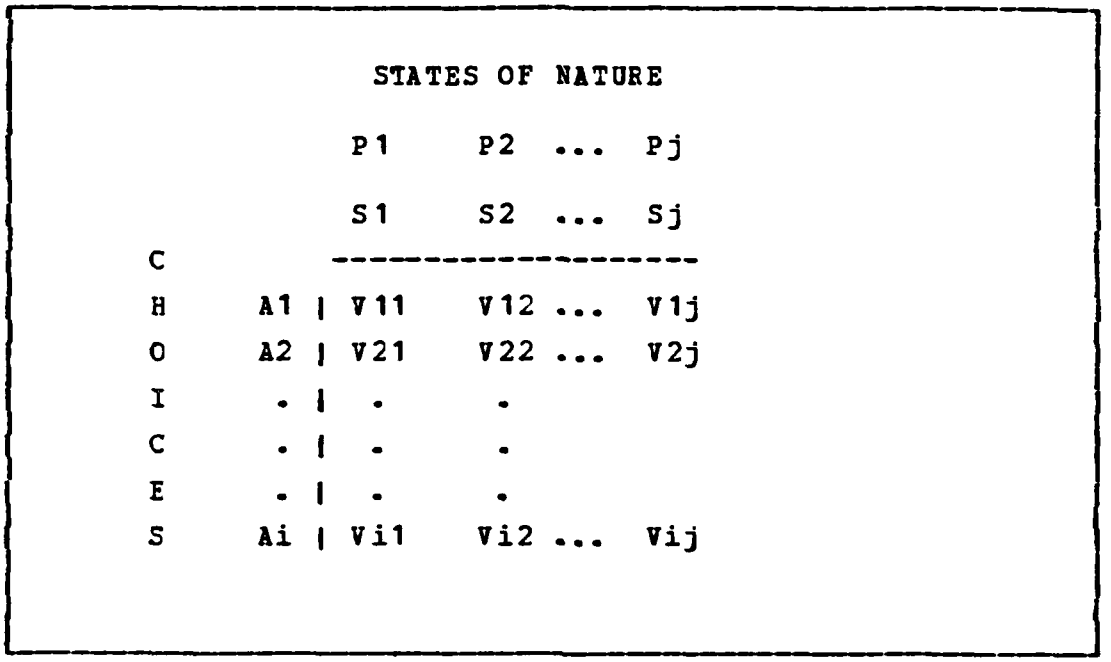

Figure 2.3 A Sample Decision Matrix

III. ENVIRONMENTAL DATA

IREPS analysis of data collected by United States carriers operating in the Eastern Mediterranean and Northern Arabian Seas has been useful in providing the actual frequency of occurrence and positions of anomalously refractive layers in these areas of operations. These data were used to create realistic test scenarios for this study. The following sections are a summary of the meteorological results.

A. EASTERN MEDITERRANEAN SEA

During a deployment cruise in 1983, the USS Eisenhower (CVN-69) collected and analyzed radiosonde data for a period from August through November while on station in the Eastern Mediterranean Sea. Soundings were taken from the aircraft carrier twice a day when feasible, generally around 0000z and 1200z. IREPS analysis of the environmental data showed that elevated trapping layers occurred 73% of the time. The ducts were most commonly found between 1,000 ft and 5,000 ft, with a mean of 2,700 ft and a standard deviation of 2,480 ft. Figure 3.1 provides a boxplot of the density of the altitudes for the elevated ducts for each month. The boxplots have an interquartile range (IQR) of 50%. The IQR represents the altitudes of approximately half the ducts observed. The data are arranged so that 25% are below the lower quartile and 25% of the data are above the upper quartile. An outlier for the environmental data set would represent a duct that is more than one IQR from the upper or lower quartile [Ref. 10]. On occasion, ducts were noted as high as 15,000 ft. The frequency of occurrence for the

elevated ducts at each altitude and during each month are shown in Figure 3.2 . Trapping layers were found to occur about 60% of the time at 5,000 ft. The higher altitudes had a lower percent of occurrence.

Subrefractive layers had an occurrence rate of 50% and were frequently found between 5,000 ft and 15,000 ft with a mean of 6,480 ft and a standard deviation of 6,310 ft. Only on rare occasions were subrefractive layers noted above 20,000 ft. Figure 3.3 provides a boxplot showing the density for subrefractive layer altitudes. The frequencies of occurrence of subrefractive layers for each altitude during a month are found in Figure 3.4 . From the environmental data it was found that subrefractive layers occurred at least 30% of the time at 5,000 ft during the sampling period. Altitudes higher than 5,000 ft had a smaller percent of occurrence. The environmental data also revealed that a larger percent of ducts occurring at altitudes above 5,000 ft was found during the month of November.

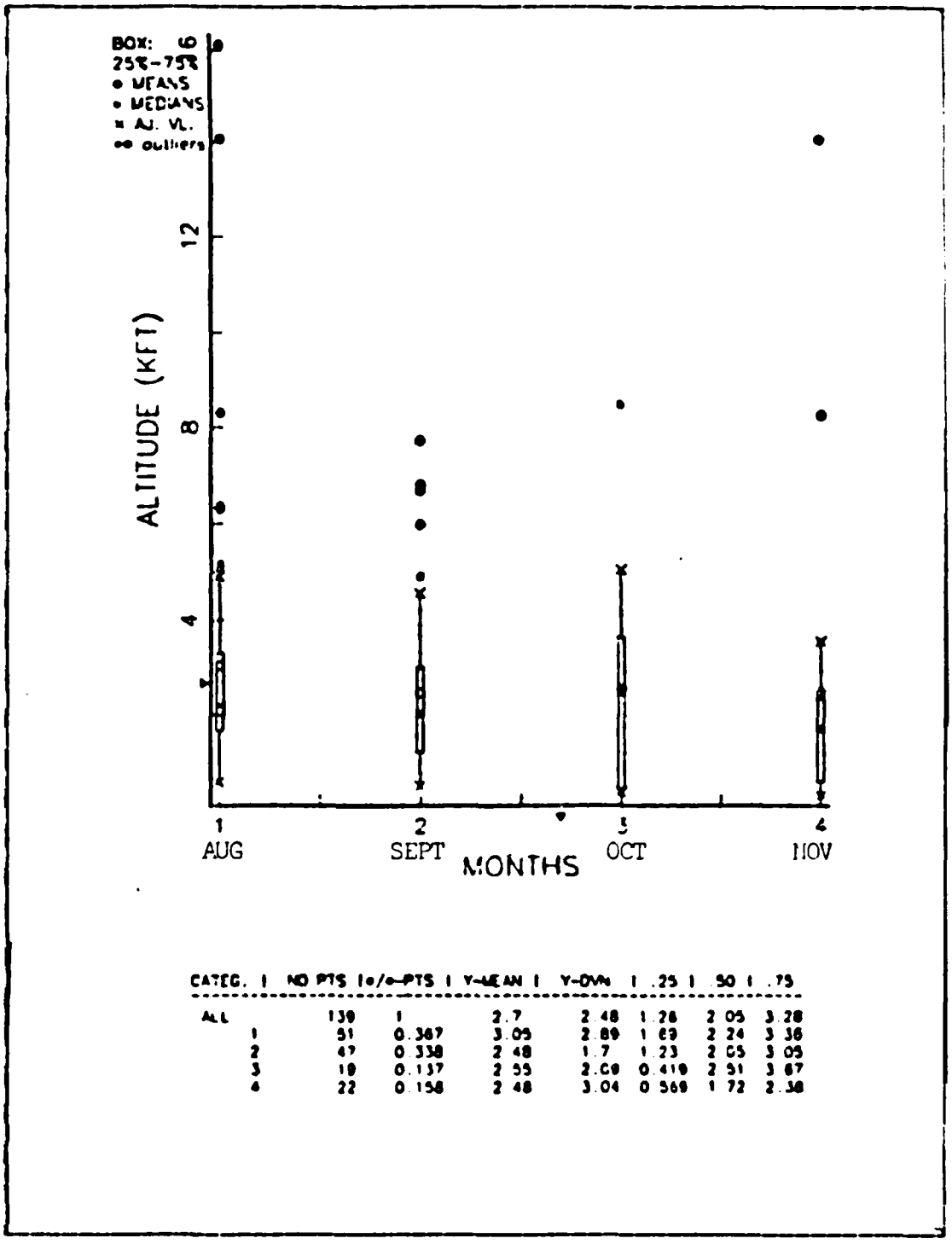

CATEG.	NO PTS	%/o-PTS	Y-MEAN	Y-DVN	.25	.50	.75
ALL	139	1	2.7	2.48	1.26	2.05	3.28
1	51	0.367	3.05	2.89	1.69	2.24	3.36
2	47	0.338	2.48	1.7	1.23	2.05	3.05
3	19	0.137	2.55	2.09	0.419	2.51	3.87
4	22	0.158	2.48	3.04	0.569	1.72	2.38

Figure 3.1 Boxplot of Elevated Duct Data

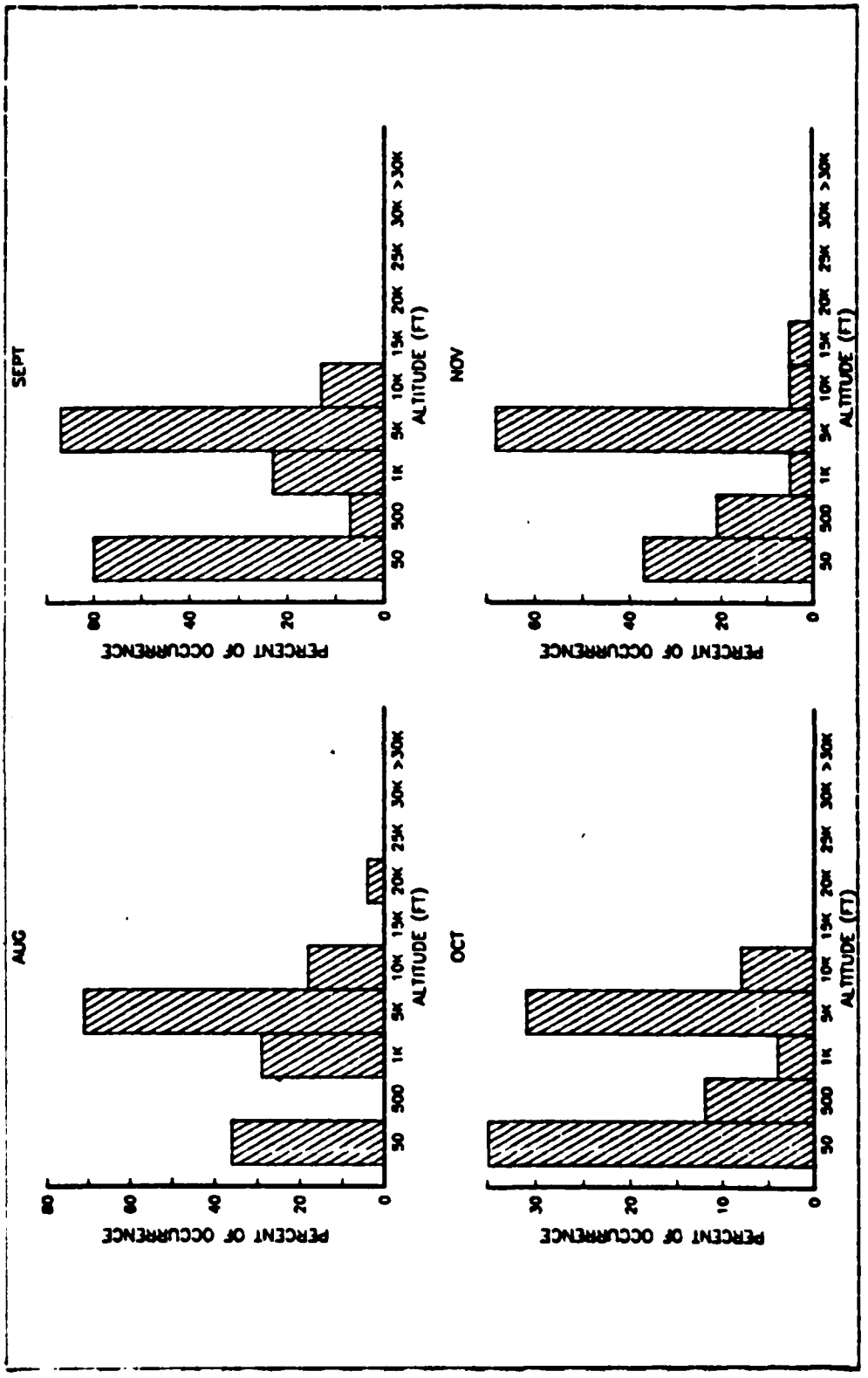

Figure 3.2 Frequency of Trapping Layers (Med)

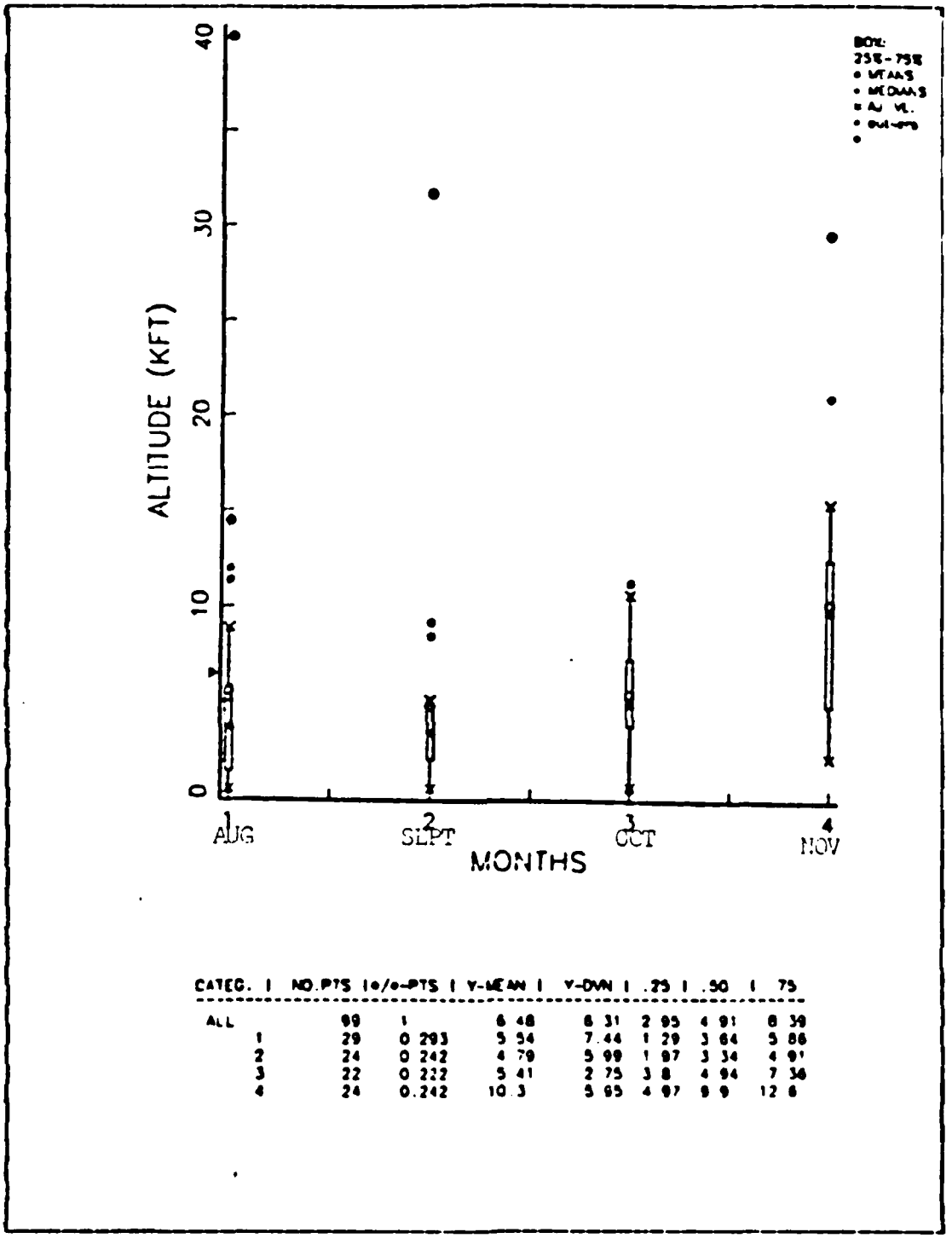

CATEG.	NO.PTS	%-PTS	Y-MEAN	Y-DVN	.25	.50	.75
ALL	99	1	6.48	8.31	2.95	4.91	8.39
1	29	0.293	5.54	7.44	1.29	3.84	5.86
2	24	0.242	4.79	5.99	1.87	3.34	4.91
3	22	0.222	5.41	2.75	3.8	4.94	7.36
4	24	0.242	10.3	5.65	4.87	8.9	12.8

Figure 3.3 Boxplot of Subrefractive Layer Data (Med)

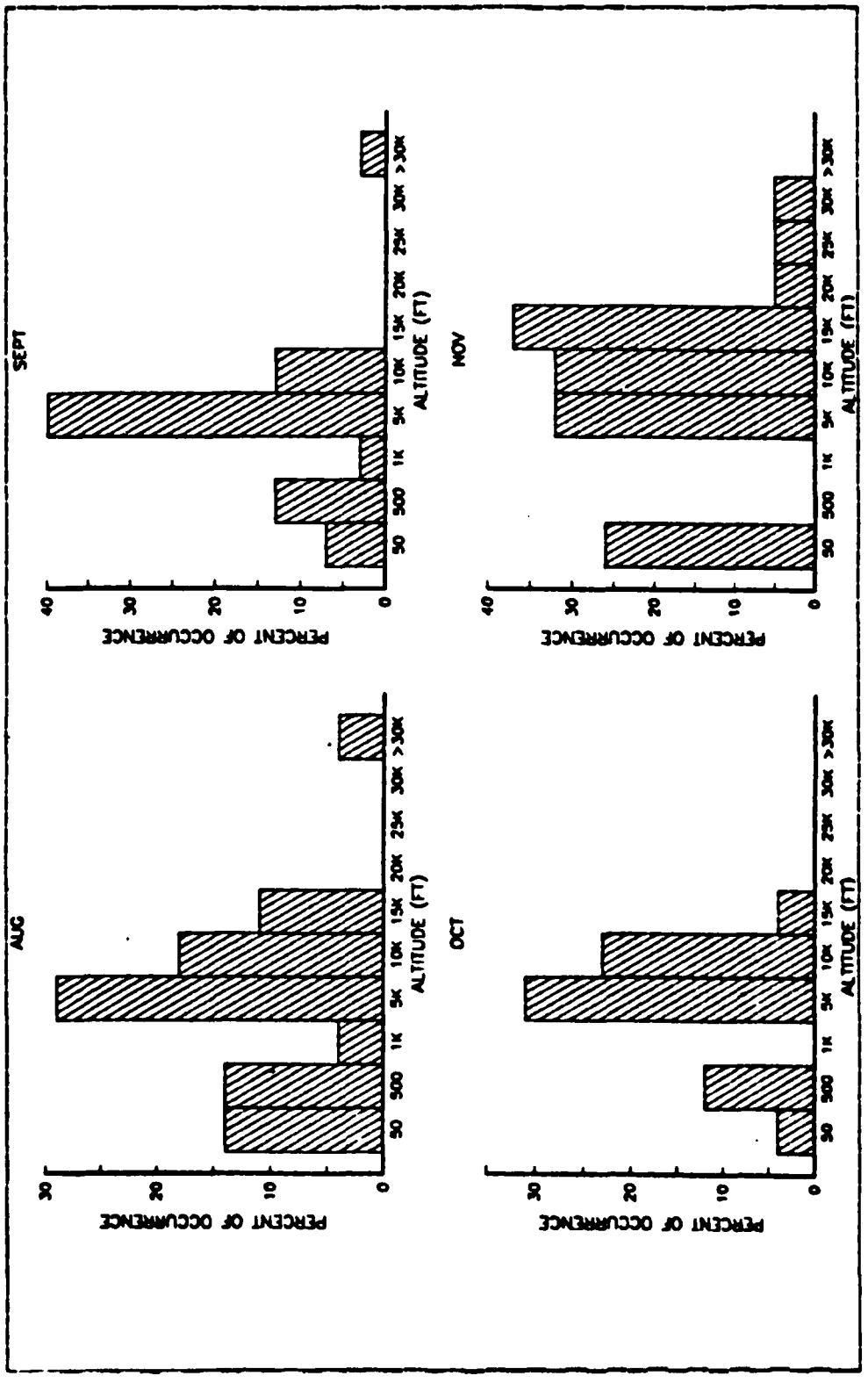

Figure 3.4 Frequency of Subrefractive Layers (Med)

Multiple layers and combinations of layers were found in the environmental data. The results of the data showed that multiple trapping layers, consisting of two or more ducts, were observed 25% of the time. Multiple subrefractive layers had an occurrence rate of 20%. Combinations consisting of both subrefractive layers and elevated ducts were observed 35% of the time. Table 2 shows the results of the separations between the multiple layers.

TABLE 2
Composition of Multiple Layers

Multiple Layers (Top-Bot)	Separations (ft) Min	Max	Avg	St. Dev.
Sub-Sub	160	13,883	3,574	1,669
Elev-Elev	114	15,126	1,882	1,422
Elev-Sub	204	14,833	2,245	814
Sub-Elev	293	10,942	3,625	2,510

B. NORTH ARABIAN SEA

Data for the Northern Arabian Sea were collected and analyzed by the USS Kennedy (CV-67) while deployed in this area from February through April of 1982. IREPS analysis of

the environmental data collected from the radiosondes revealed that elevated ducts occurred in the area 65% of the time. The ducts were generally formed between 2,000 ft and 7,000 ft with a mean of 3,840 ft and a standard deviation of 2.07 kft. A boxplot and a frequency count of the trapping layers is represented in Figures 3.5 and 3.6 . During the deployment, altitudes around 5,000 ft had the highest occurrence of trapping layers which ranged between 30% and 70%. Altitudes higher than 5,000 ft occurred less frequently. Information about the subrefractive layers was not available.

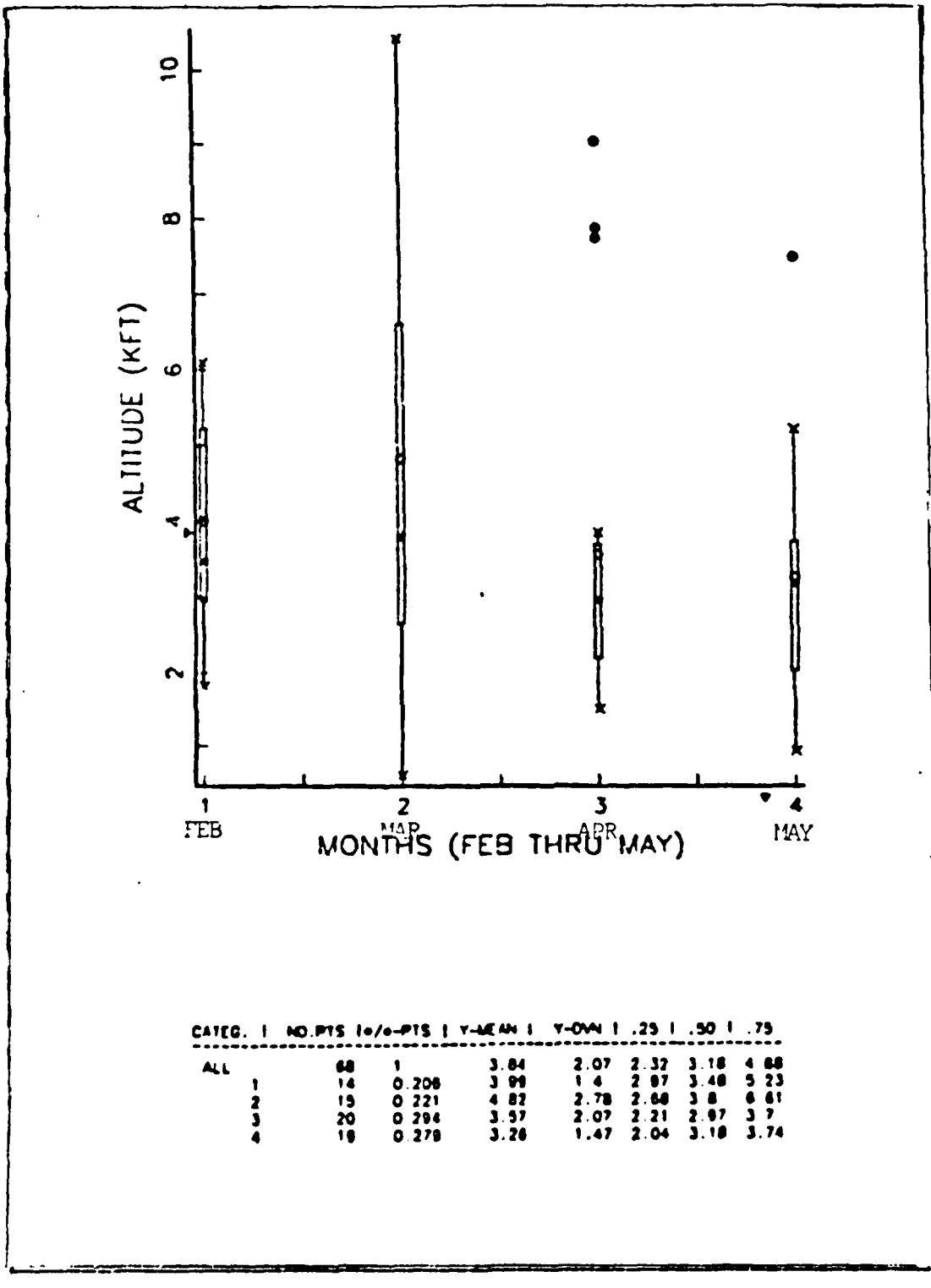

CATEG.	NO.PTS	%/o-PTS	Y-MEAN	Y-DVN	.25	.50	.75
ALL	68	1	3.84	2.07	2.32	3.18	4.68
1	14	0.206	3.99	1.4	2.87	3.48	5.23
2	15	0.221	4.82	2.78	2.68	3.8	6.61
3	20	0.294	3.57	2.07	2.21	2.97	3.7
4	19	0.279	3.26	1.47	2.04	3.18	3.74

Figure 3.5 Boxplot of Trapping Layer Data (NAS)

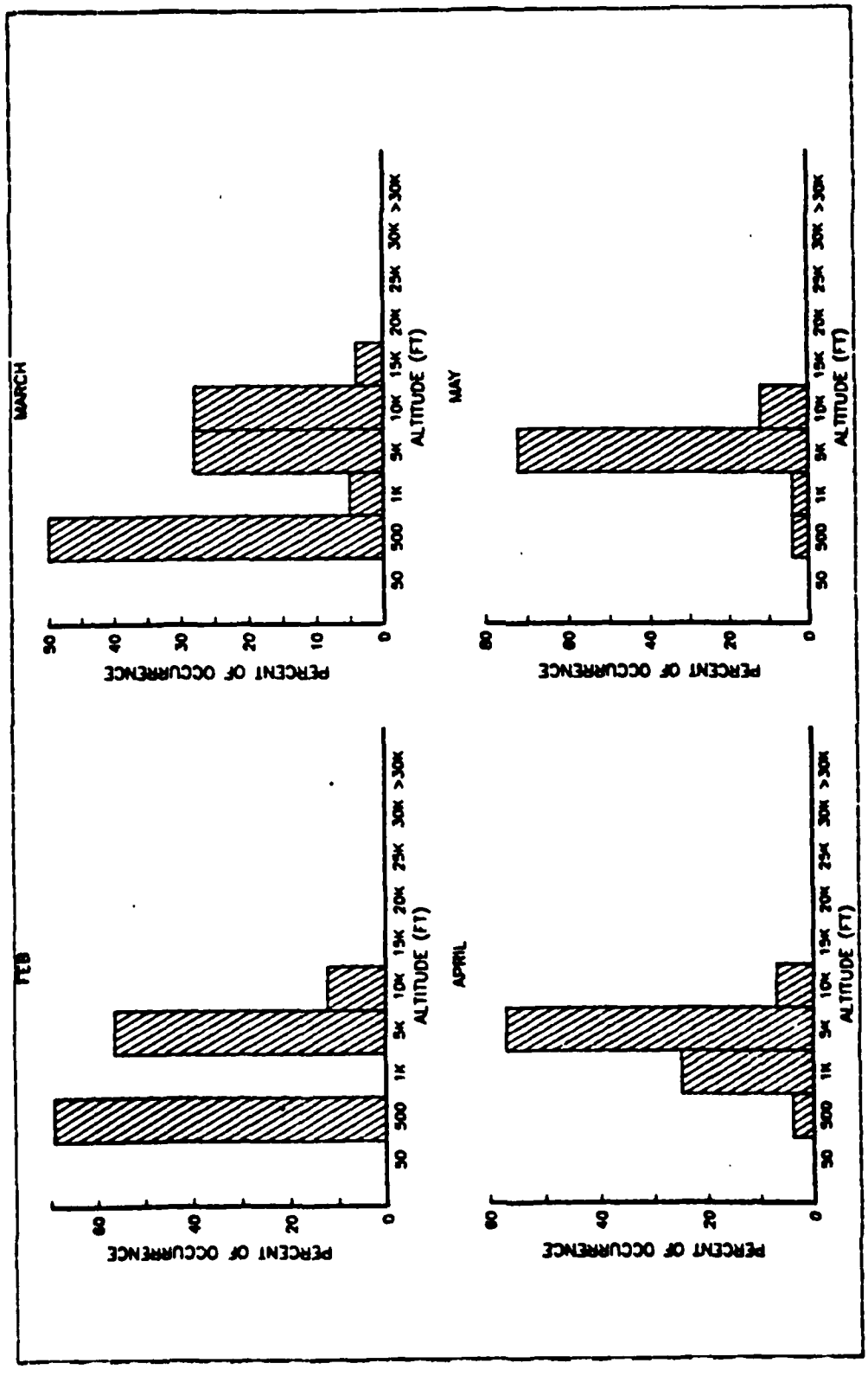

Figure 3.6 Frequency of Trapping Layers (NAS)

IV. SUBREFRACTIVE LAYERS

From the information gained through the environmental data analysis, several scenarios were created and modeled by IREPS program to determine the effects that a subrefractive layer has on an aircraft's radar propagation and on a non-radiating aircraft's ability to receive the transmission of EM waves. The IREPS model uses ray tracing to simulate radar propagation. Radar reflections off the earth's surface, which may lead to an improved radar coverage, are not represented in the results. For the purpose of this study, the frequency of the airborne radar was set at 450 MHz. Higher frequencies will experience greater refraction [Ref. 11]. A combination of the following characteristics were used to develop several possible subrefractive scenarios:

Gradients: +30, +60 N units/kft

Altitudes: 5,000, 10,000, 15,000, 20,000, 25,000 ft.

The thickness of the subrefractive layer was varied at 100, 200, and 300 ft.

Once the environmental data were determined for each scenario, the aircraft was then positioned below, in, and above the subrefractive layer. An analysis for each of the scenarios consisted of determining the measures of effectiveness related to each example (see Methodology for MOEs).

Airborne early warning and surveillance encourages maximizing radar coverage and early warning distance by reducing any negative atmospheric effects. The constraints associated with this objective include the the aircraft's

ceiling limitation and the radar source's maintaining a minimum altitude to achieve a desired distance to the radar horizon.

A. SUBREFRACTIVE LAYER EXAMPLE

The environmental profile shown in Table 3 was created to demonstrate the effects of a subrefractive layer on an airborne radar.

TABLE 3
Environmental Data List

Subrefractive layer +60 N units/kft

Level	Feet	N units	M units	N/kft	Condition
1	0.0	350.0	350.0		
				-11.8	Normal
2	14,800	175.4	883.4		
				+60.0	Sub
3	15,000	187.4	905.0		
				-11.8	Normal
4	30,000	10.4	1,445.6		

The subrefractive layer example is at an altitude of 15,000 ft (top of layer), 200 ft thick and has a gradient change of +60 N units/kft from the normal gradient of -11.8 N units/kft. The radiating aircraft was then positioned at several altitudes with relationship to the refractive layer.

B. RESULTS OF THE SUBREFRACTIVE LAYER SCENARIO

When the radar is positioned below the subrefractive layer, the IREPS model indicates that normal radar coverage is experienced by the aircraft. A sensitivity analysis of radar altitudes below subrefractive layers reveals that the aircraft need only fly 100 ft below the layer and normal radar coverage will exist (see Appendix A, Figure A.2). Table 4 is a summary of the measures of effectiveness, calculated from the IREPS graphical output, for the subrefractive layer example when the radar is positioned in and above the layer.
The aircraft was found to experience normal radar coverage at 14,700 ft which is 100 ft below the layer. It is also noted that when the aircraft was positioned at 25,000 ft or higher (a height greater than 10,000 ft above the layer) IREPS revealed no significant effect on the radar coverage by the subrefractive layer. The graphical results of the subrefractive layer are shown in Figure 4.1 .

A summary of the findings for a radiating source when a known subrefractive layer is present are as follows:

a) If the aircraft is positioned approximately 100 ft below a subrefractive layer or lower, this is sufficient separation to provide normal radar coverage (see Appendix A, Figure A.2).

b) If the aircraft is positioned in the subrefractive layer, an area of potential radar distortion caused by wave bending will form and a loss in signal strength inside the area may be experienced (see Appendix A, Figure A.3).

c) If the aircraft is positioned above the subrefractive layer, the aircraft should fly as high above the layer as possible. By increasing the height of the aircraft above the

TABLE 4

Results of MOEs for a Subrefractive Layer

Altitude 15,000 ft, 200 ft thick and
a refractive gradient of +60 N units/kft

Alt. aircraft (ft)	Δa (ft) from layer	Dist (Nm) Radar Anomaly	Area (Nm^2) Radar Anomaly	Dist (Nm) Radar Horizon
14,700	below	None	None	149.1
14,900	In	20.0	97.5	150.1
15,000	top	21.5	96.7	150.6
16,000	1,000	38.9	80.6	155.6
17,000	2,000	55.0	30.2	160.4
18,000	3,000	67.4	24.9	165.0
19.000	4,000	77.8	20.4	169.5
20,000	5,000	87.0	18.8	173.9
25,000	10,000	123.0	9.1	194.5
30,000	15,000	None	None	213.0

layer, the area of the radar distortion diminishes and is located further away from the radar source (see Appendix A, Figures A.4, A.5 and A.6). At altitudes above 25,000 ft, IREPS indicated the anomalous effects on the radar waves had little significance.

These findings from the IREPS simulation did not consider radar reflections off the earth surface which may help to improve the radar coverage.

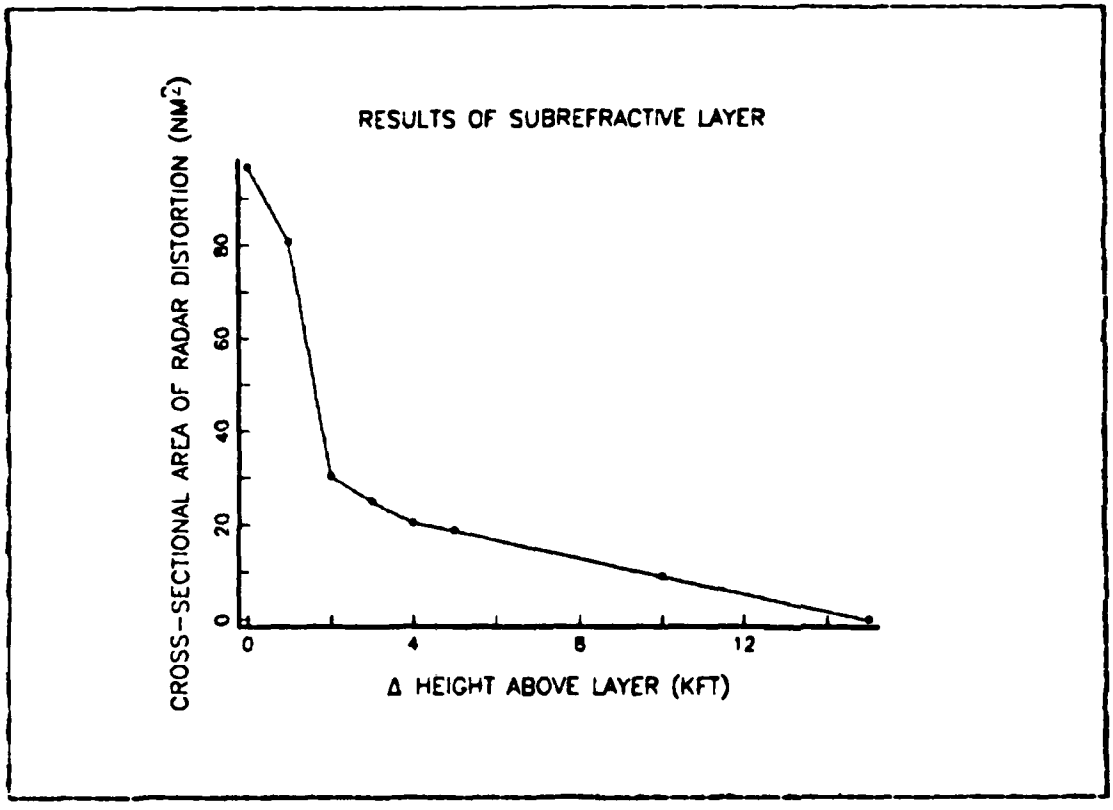

Figure 4.1 Subrefractive Layer Graphical Results

C. DECISION MATRIX FOR SUBREFRACTIVE LAYER

Based upon the principles of decision theory, a matrix can be constructed from the information to aid in determining possible flight profiles. The states of nature will be the altitudes where the subrefractive layers may exist. They will be labled Sj for each j subrefractive layer. The decision alternatives will consist of the possible flight altitudes of the radiating source. The alternatives will be labled Ai for each i flight altitude of the aircraft. The payoff values for the matrix will consist of relative radar coverage conditions which were selected from the graphical results of the subrefractive layer. A combination of the change in height above the

refractive layer and natural breaks in the subrefractive layer results curve were used to determine the boundaries for the radar coverage conditions. The categories of radar coverage are described by the position of the radar source to the layer and the corresponding cross-sectional area of radar distortion that results from the anomalous propagation of the EM waves. For the purpose of this matrix the following definition of radar conditions will be used.

A = category A; normal radar coverage exists. This occurs when the radar is either ≥ 100 ft below the subrefractive layer or > 10,000 ft above the layer. This also equates to a cross sectional area of distortion < 10 nm^2.

B = category B; the altitude of the aircraft is 5,000 ft to 10,000 ft above the subrefractive layer (10 nm^2 ≤ cross-sectional area of distortion < 20 nm^2).

C = category C; the altitude of the aircraft is 1,000 ft to 5,000 ft above the layer (20 nm^2 ≤ cross-sectional area of distortion ≤ 80 nm^2).

D = category D; the aircraft is radiating in or less than 1,000 ft above the layer (cross sectional area of distortion > 80 nm^2).

Using the radar coverage categories for a subrefractive layer as payoff values, a decision matrix was constructed (see Figure 4.2). The states of nature for the subrefractive layers in this decision matrix range from 5,000 ft to 30,000 ft. The alternative decision altitudes, go from 4,000 ft to 25,000 ft.

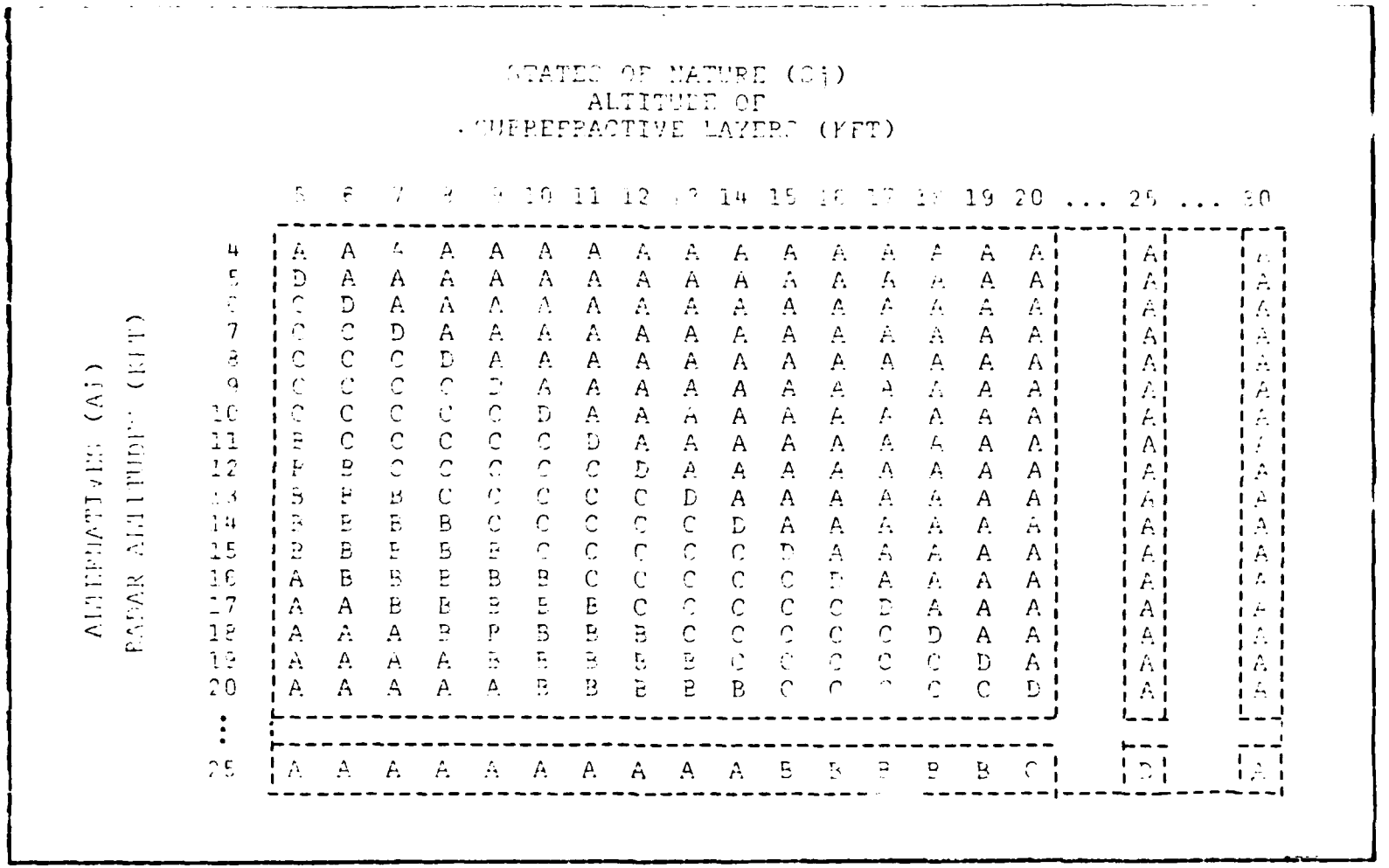

Figure 4.2 Decision Matrix for a Subrefractive Layer

One assumption in the decision matrix is that the radiating source or ESM aircraft will be equipped with an airborne microwave refractometer or radiosonde data will be available and as a result the states of nature will be known. Given the information about the state of nature, the aircraft would fly at an altitude that could provide a profile with potentially a category A radar coverage. This will occur when the aircraft flys below the subrefractive layer, as shown by the upper right portion of the decision matrix (see Figure 4.2). However, The subrefractive layer may exist at an altitude where, in order for the radiating aircraft to achieve a category A profile, the radar must be positioned at an altitude with a less than desirable distance to the radar horizon. The aircraft may then be willing to accept a category B radar coverage and an increased radar horizon. The decision matrix for the subrefractive layer may be converted to a graphical representation, as shown in Figure 4.3, for further assistance in the decision.

The graphical decision aid on the subrefractive layer is used in the following manner:

1. Draw a line parallel to the flight altitude axis where the known subrefractive layer exists.

2. Proceed along the altitude line of the subrefractive layer until it intersects the area of category D coverage.

3. Locate the flight altitude of this intersection. If the flight altitude is high enough for the desired radar horizon, then fly at 100 ft below this altitude so the aircraft is below the layer.

4. If the altitude does not provide for an adequate radar horizon, continue along the altitude line of the

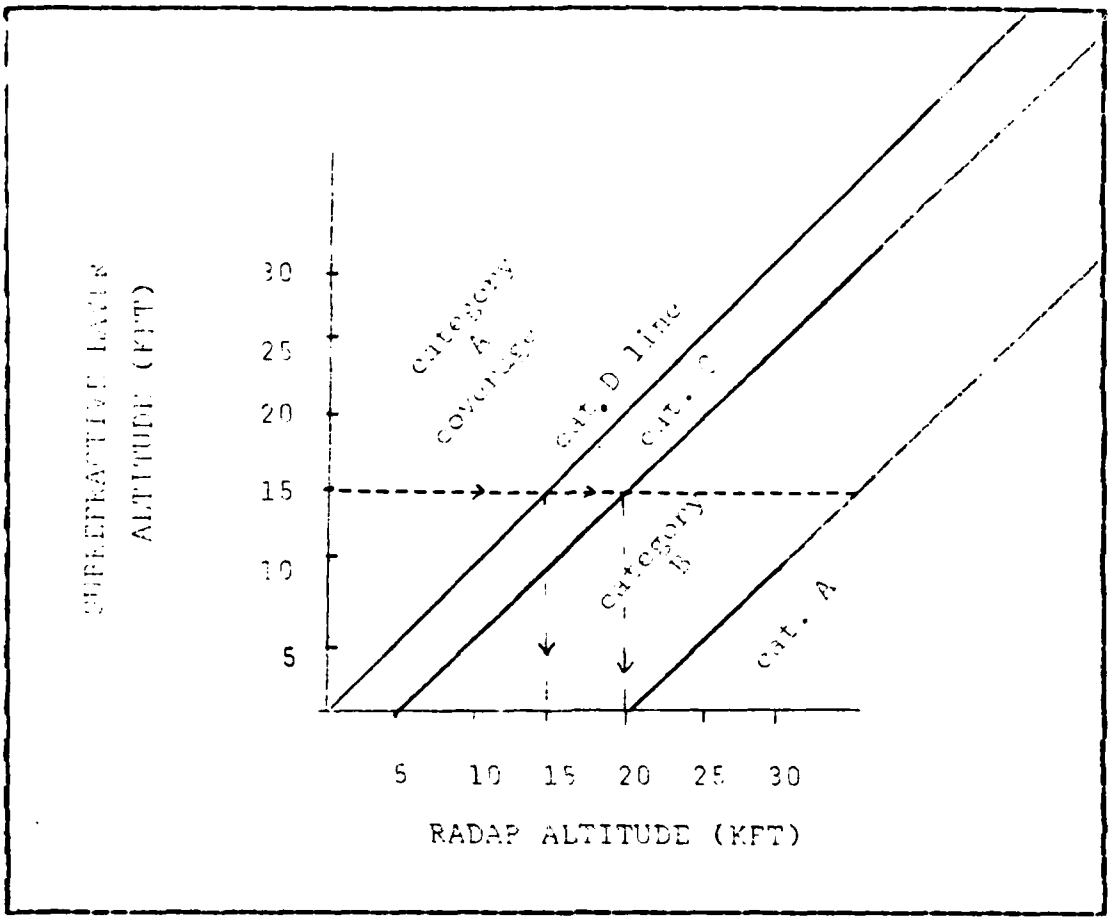

Figure 4.3 Subrefractive Layer Graphical Tool

subrefractive layer until both a coverage area and a radar horizon associated with the aircraft's altitude is acceptable to the decision maker.

D. DISCUSSION ON SUBREFRACTIVE LAYERS

The analysis of the possible effects a subrefractive layer has on an aircraft's radar has offered some insight into the placement of the aircraft. Where an aircraft is positioned is highly dependent upon its mission (e.g. active

coverage, passive ESM or covert). The following comments address both a radiating aircraft and a non-radiating aircraft.

1. Radiating Aircraft

The results from the IREPS model reveal that the best option for an aircraft's use of its radar is to fly below the subrefractive layer if the radar horizon is sufficient. If the radar horizon is not acceptable and it is necessary to fly above the layer, the aircraft should position itself as high above the layer as practical to avoid potential loss of signal at some altitudes and ranges.

2. Non-radiating Aircraft (ESM)

The optimal flight profile (altitude) of an ESM aircraft is a function of the relationship between the altitude of the EM source, the height of the subrefractive layer, and the range to the EM source.

a) If the EM source is known to be radiating below the subrefractive layer, there is no apparent effect on the its electromagnetic emissions and the ESM aircraft can fly at any height above the minimum line of sight altitude (see Appendix A, Figure A.2).

b) If the EM source is radiating in or above the subrefractive layer, the ESM aircraft should generally fly at a flight profile that considers other contributing factors (e.g. fuel, communications, etc.) and be aware of possible areas where the signal received may be less than for normal propagation. The degraded signal area will change altitudes as the ESM aircraft increases or decreases its range to the EM source (see Appendix A, Figure A.3).

c) If a non-radiating aircraft wishes to remain hidden from the radiating source, it should try to remain inside the subrefractive layer or immediately below the layer. This practice works especially well when the refractive layer is formed close to the ground and causes the search radar's waves to be bent away from the covert aircraft. Figure 4.4 demonstrates that an AEW aircraft's ability to detect low flying aircraft is hindered by a subrefractive layer. The AEW aircraft must position itself closer to the coast or at a higher altitude in order that its radar waves have a sufficient angle to penetrate the layer. The range at which the AEW aircraft first detects the covert aircraft will be at a closer distance than under normal conditions at sea [Ref. 12].

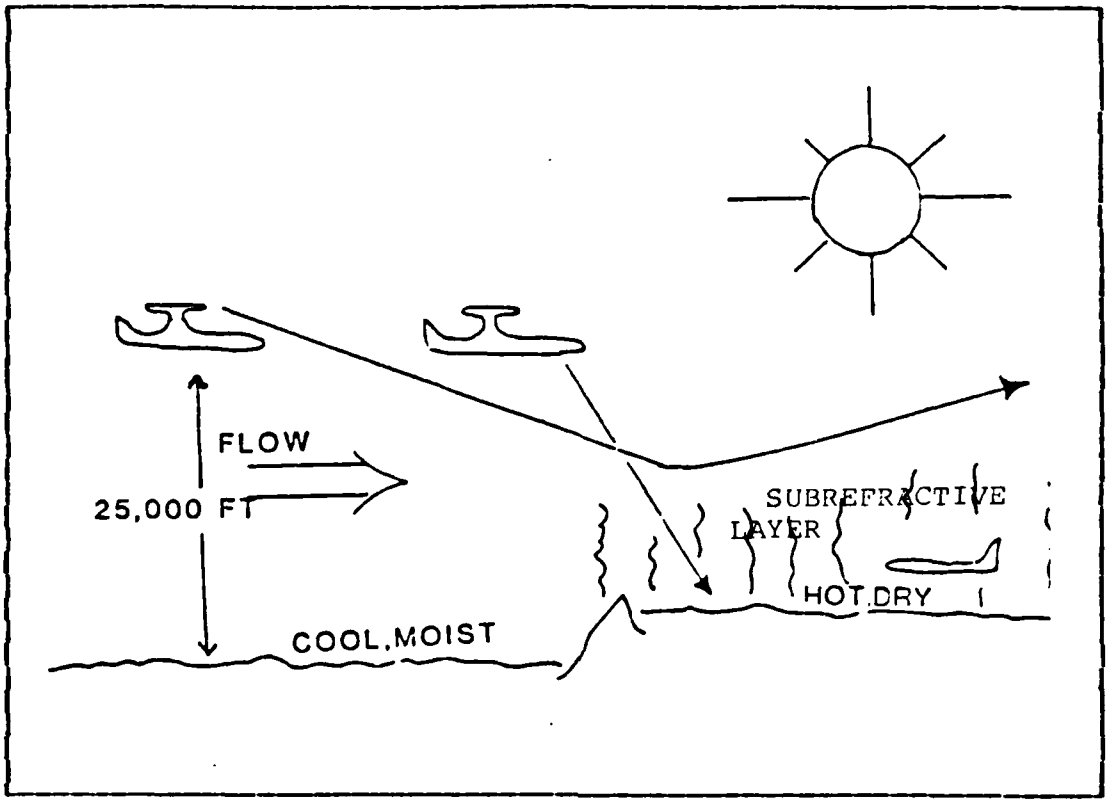

Figure 4.4 Subrefractive Layer Close to the Surface

V. ELEVATED DUCTS

Stable summer weather with clear skies and light winds provides an ideal setting for the existence of strong ducts over the ocean. One of the primary causes of elevated trapping layers is the temperature inversions produced by the presence of warm dry air over a region of cooler moist air (see Figure 5.1).

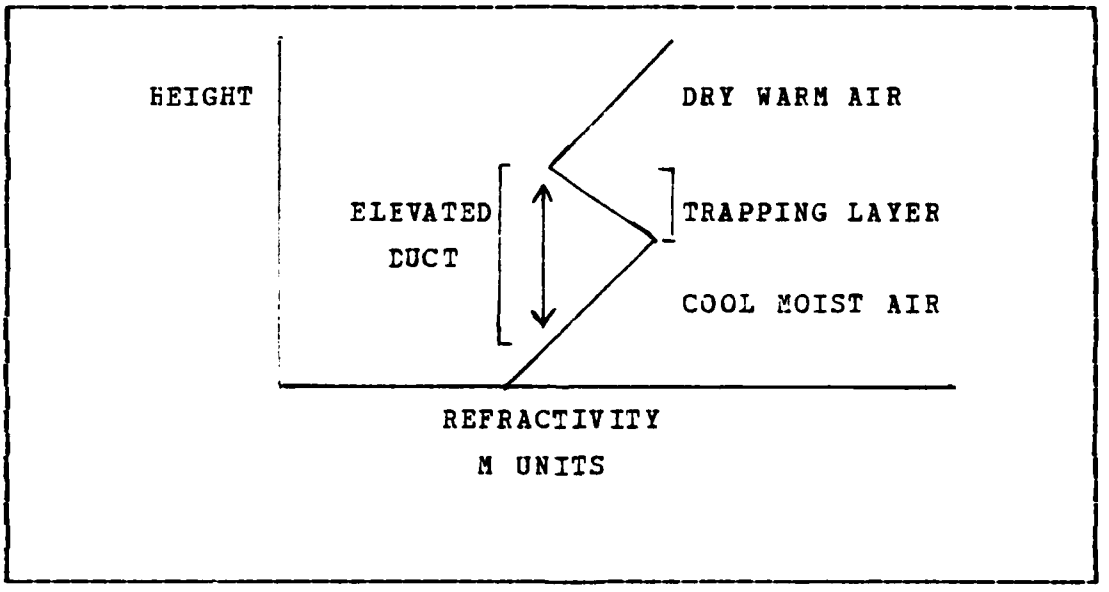

Figure 5.1 Description of an Elevated Duct

Because of the necessary meteorological conditions, the elevated ducts are most commonly found in the lower latitudes, North Arabian Sea, Mediterranean Sea, Caribbean Sea and Central Pacific [Ref. 7 p. 93]. Generally, the elevated ducts will form below 5,000 ft, but they can occur as high as 15,000 ft. The thickness of a duct is

significant. As in a wave guide, a certain minimum thickness is required to propagate a specific radio wavelength. The relationship of the EM frequency to minimum duct thickness is shown in Table 1 of Chapter II.

Elevated ducts, primarily, have a significant impact on air-to-air operations including early warning (AEW), surveillance, communications and weapons guidance systems. Elevated ducts can contribute to extended ranges of communications and surveillance if both the transmitting and receiving sources are co-located in the duct. However, also associated with ducting is the existence of large areas with diminished probability of detection, often referred to as radar holes or radar fading, located above the trapping layer. To evaluate the effects elevated ducts have on an aircraft's EM transmission and reception, several atmospheric profiles were designed and tested using the IREPS model from a combination of the following parameters:

Gradient: -48, -90, -200, -400 (N units/kft) Note: The larger negative gradient yeilds a stronger duct.

Thickness of duct: 100, 200, 300, 400 (ft)

Elevation of duct top: 5,000, 10,000, 15,000 (ft)

Radar frequency: 450 MHz

The test and evaluation of each scenario was conducted in a similar manner to the analysis of the subrefractive layer example. The radar source was positioned at various heights with relationship to the altitude of the duct. The object of each trial was to maximize radar coverage and early warning detection.

A. ELEVATED DUCT EXAMPLE

The following is the environmental data of an elevated duct located at 10,000 ft , 300 ft thick and a refractive gradient change of -90 N units/kft (see Table 5). These parameters were selected for the test example since they created a duct that posed a tactical problem to an AEW aircraft and had the proper thickness to propagate a 450 MHz signal.

TABLE 5
Environmental Data List

Elevated duct -90 N units/kft

Level	Feet	N units	M units	N/kft	Condition
1	0	350.0	350.0		
				-11.8	Normal
2	9,850	233.8	705.0		
				-90.0	Trap
3	10,000	220.3	698.7		
				-11.8	Normal
4	25,000	43.3	1,239.3		

B. RESULTS OF ELEVATED DUCTS

By varying the altitudes of the radar source in relationship to the trapping layer, the MOE results in Table

6 were obtained. These results were calculated from the IREPS graphical output according to the stated measures of effectiveness.

TABLE 6
Results of Elevated Duct MOEs

Alt. aircraft (ft)	Δa (ft) from layer	Dist. (nm) Radar Anomaly	Area (nm^2) Radar Anomaly	Dist. (nm) Radar Horizon
9,500	below	none	none	119.9
9,700	in	35.0	41.3	121.1
9,900	in	20.0	142.5	122.4
10,000	top	14.0	170.5	123.0
11,000	1,000	38.9	80.6	129.0
12,000	2,000	55.0	60.4	134.7
13,000	3,000	67.4	52.5	140.2
14,000	4,000	77.8	40.7	145.5
15,000	5,000	87.0	35.3	150.6
16,000	6,000	93.5	30.4	155.6
17,000	7,000	102.9	28.3	160.4
18,000	8,000	110.0	24.4	165.0
19,000	9,000	116.7	20.8	169.5
20,000	10,000	123.0	16.0	173.9
25,000	15,000	150.6	8.2	194.5
30,000	20,000	none	none	213.0

As indicated by the IREPS output, the radar source experienced no anomalous propagation at altitudes less than or equal to 9,600 ft which was about 100 ft below the trapping layer. Extended ranges of EM waves, due to trapping, occurred between 9,700 ft and 10,000 ft. Radar fading existed when the radar source was positioned in or above the duct. The area of radar distortion decreased in size with an increase in height above the layer. Normal radar coverage resumed at 30,000 ft. From the results on the elevated duct example in Table 6, a graph of the measured vertical cross-sectional area of the radar distortion (nm^2) and the change in height above the trapping layer (ft) was plotted (see Figure 5.2). Radar wave reflections off the surface of the earth are not considered in the IREPS results.

C. DECISION MATRIX FOR ELEVATED DUCT

Based upon the information from Figure 5.2, areas of radar coverage were defined by the radar source position relative to the duct and the radar distortion cross-sectional area. The quality of the coverage was catergorized as follows:

A = category A; normal radar coverage. Radar source located below the duct or at an altitude greater than or equal to 15,000 ft above the elevated duct. This also equates to a radar distortion cross-sectional area less than 10 nm^2.

B = category B; radar source positioned between 10,000 and 15,000 ft above the trapping layer. Radar cross-sectional area between 10 and 20 nm^2.

C = category C; radar source positioned between 3,000 and 10,000 ft above the duct. Radar cross-sectional area between 20 and 50 nm^2.

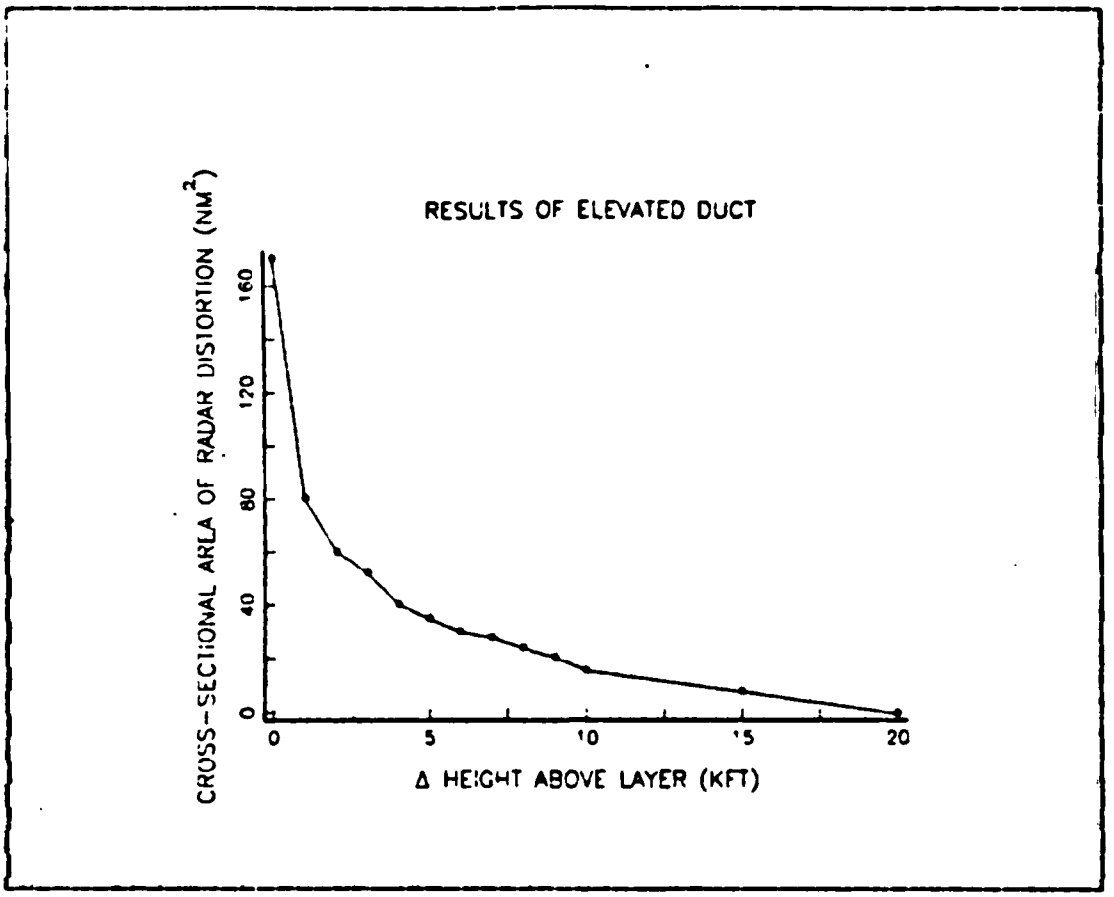

Figure 5.2 Graphical Results of Elevated Duct

D = category D; radar source positioned between the top of the duct and 3,000 ft above the layer. Radar cross-sectional area between 50 and 170 nm².

DX = category D with extended ranges. Radar source is positioned in the duct and experiences both an extended radar range for the altitude of the duct and an area of radar fading above the duct.

From the information about the elevated duct scenarios, a decision matrix can be constructed similarly to the decision matrix for the subrefractive layer. The states of nature in

this case will consist of the heights associated with the trapping layers and the choices for the alternative decisions will be the possible altitudes for positioning the radar source. The payoff values for the decision matrix will be the category of the radar coverage. The construction of this decision matrix is based upon the assumption that the position of the trapping layer will be known. This will be true when the aircraft is equipped with an airborne microwave refractometer or radiosonde data are available. The altitude for the states of nature will describe the top of the duct. The decision matrix for the elevated duct example is shown in Figure 5.3 .

As demonstrated by both the results and the decision matrix, an area of category A radar coverage may be achieved if the radiating source is located below the duct. However, flying at an altitude below the trapping layer may not provide for an adequate distance to the aircraft's radar horizon. As in case of the subrefractive layer this is a two step decision process, the aircraft may elect to fly above the duct in an area described as category B radar coverage and increase its radar horizon. The decision matrix has been transformed into a graphical representation for use as an additional decision aid (see Figure 5.4). Similar procedures apply to the use of this graph as were applied to the decision graph for the subrefractive layer example. First locate the altitude of the existing duct and then draw a line parallel to the axis of the radar source altitude. Next, determine a point on the line that provides adequate radar coverage and maintains a desired distance to the radar horizon, then fly at an altitude that corresponds to that point.

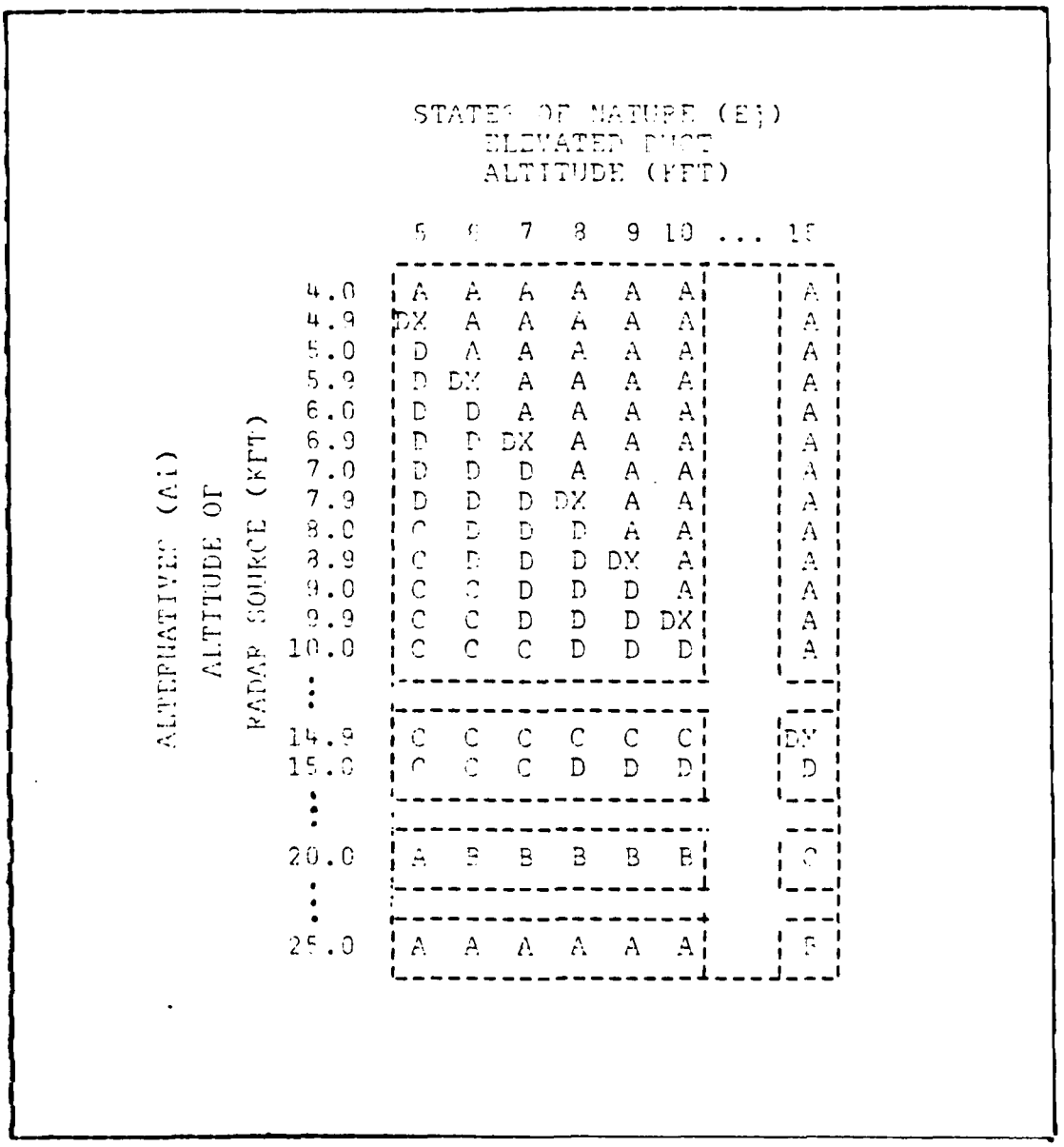

Figure 5.3 Decision Matrix for Elevated Duct

D. ANALYSIS OF ELEVATED DUCT SCENARIO

The information obtained about elevated ducts from the IREPS model have led to the following analysis about the positioning of radiating and non-radiating aircraft in an atmosphere with trapping layers.

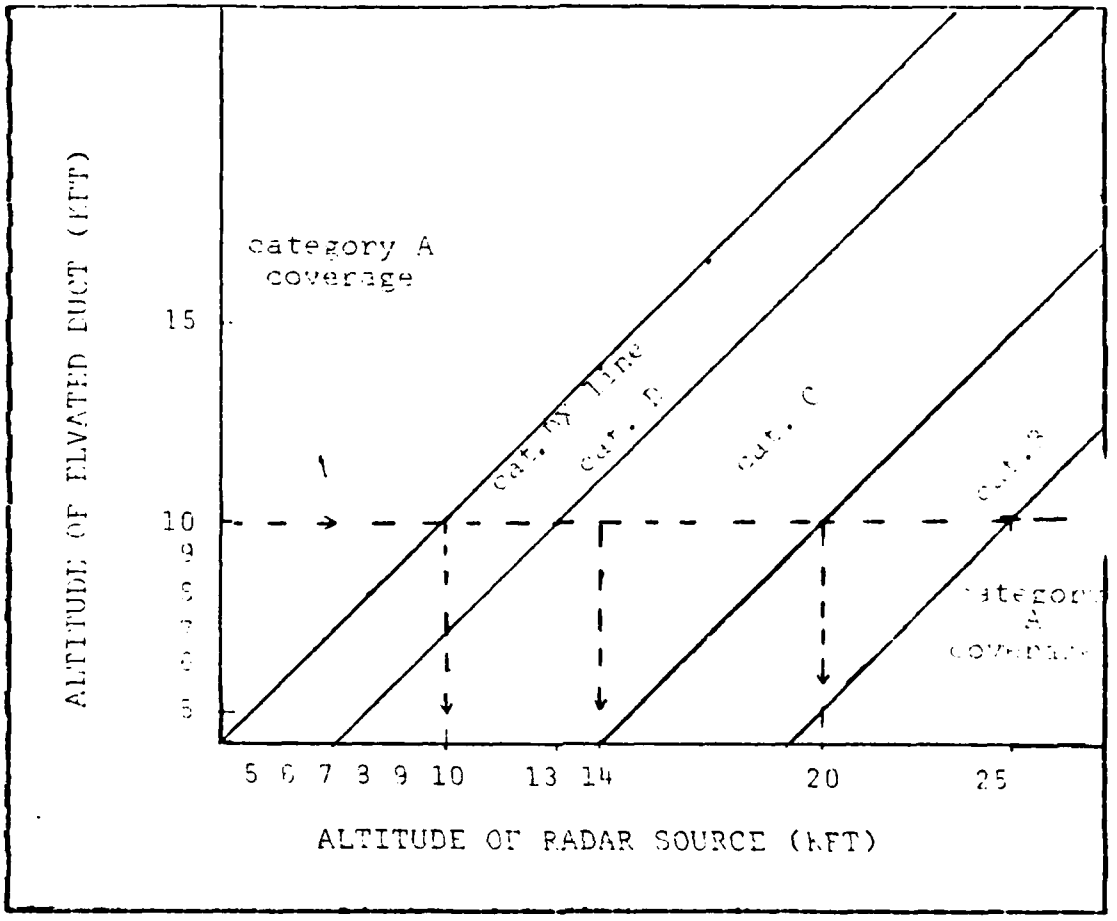

Figure 5.4 Elevated Duct Graphical Decision Tool

1. Radiating Aircraft

The follcwing information applies to the anomalous effects on the radiating source:

a) If the radar source is positioned below the duct, the aircraft experiences normal radar coverage (see Appendix B, Figure B.2).

b) If the radar source is positioned in the duct, extended EM propagation occurs at the altitude of the duct and a blind spot or area of diminished radar probability of

detection may exist above the duct (see Appendix B, Figures B.3, B.4 and B.5).

c) If the radar source is positioned immediately above the duct, IREPS indicates that the aircraft experiences its maximum area of diminished radar detection. This appears to be the least desirable altitude for a radiating aircraft conducting an air-to-air search, since the radar may experience a large area of radar fading and no extended radar ranges (see Appendix B, Figure B.6).

d) As the radar source position increases with altitude above the duct, the size of the region of radar distortion diminishes and is located further from the aircraft (see Appendix B, Figures B.7 and B.8). When the radar source was positioned above 25,000 ft, which was a change in height above the layer greater than 15,000 ft, there was no indication of anomalous effects on the radar waves.

2. Non-radiating Aircraft

The ability for an ESM aircraft to intercept a hostile aircraft's radar is complicated by the effects of the elevated ducts. Generally, a good position for an ESM platform , in an air-to-air environment, would be in or below the duct (see Appendix B, Figure B.5). If the hostile radar and the ESM aircraft are co-located in the trapping layer, the ESM aircraft could achieve an extended detection range. However, if the hostile radar is positioned above the duct, the ESM aircraft should avoid the possible areas of radar fading. The optimal search altitude will be a function of the hostile radar's position to the duct and the distance to the victim radar (see Appendix B, Figure B.7). This search altitude only considers the effects of the atmospheric propagation and does not consider fuel efficiency. If an aircraft is attempting to remain covert,

the optimal position for this aircraft is to remain in an area of diminished probability of detection which may be located above the trapping layer when the search radar is in or above the duct (see Appendix B, Figure B.5). If the ESM aircraft decides to fly above the layer, it should maintain a substantial separation from the layer and become aware of a possible radar hole where the signal reception may fade temporarily as the aircraft appproaches the radar source. These areas of potential radar fading will be a function of the altitude of the radar source and the distance to the radar (see Appendix B, Figures B.5 through B.8).

E. DISCUSSION ON ELEVATED DUCTS

From the data analysis of the climatology information collected in the Mediterranean and Northern Arabian Seas, the environmental profile used in this example on elevated ducts had a low percentage of occurrence. This example, however, was used as a test case because it posed a significant impact on typical flight altitudes of AEW and ESM aircraft. A more common environmental profile, duct existing at 5,000 ft, was also simulated on IREPS (see Appendix B, Figures B.10, B.11 and B.12). The results were consistent with the previous findings, however, the anomalous propagation of EM waves had little impact on a radiating aircraft flying at 25,000 ft (see Appendix B, Figure B.12).

VI. MULTIPLE LAYERS

Frequently, the atmosphere is composed of several anomalously refractive layers as were shown in Chapter II, Table 2. An environment consisting of multiple elevated ducts, subrefractive layers or a combination of the two will have an anomalous effect on the propagation of radar waves. IREPS test runs, to determine these effects, were conducted on atmospheres with two subrefractive layers, two elevated ducts, a subrefractive layer above a duct and a subrefractive layer below a duct. For each of the test examples, a 300 ft refractive gradient change of -90 N units/kft was used to create a duct while the subrefractive layer consisted of a 200 ft refractive gradient change of +60 N units/kft. The change in height between the layers was tested at 500 ft and 5,000 ft. Altitude separations greater than 5,000 ft for the layers appear to yield little interaction and allow for each layer to be considered individually. The following is a qualitative analysis of the results for each of the test combinations.

A. SUBREFRACTIVE-SUBREFRACTIVE

When two subrefractive layers are known to exist together in the atmosphere, each layer will contribute individually to the bending of EM waves. An airborne early warning aircraft could possibly consider each subrefractive layer's effects separately. Generally, the most significant subrefractive layer will be the layer immediately below the radar source (see Appendix C, Figure C.2). As shown in Chapter III on subrefractive layers, positioning the aircraft below any subrefractive layer will negate the

refractive effects on the radar transmission. The decision matrix constructed for a single subrefractive layer can also be used to assist in decision making in a multilayered environment (see Chapter III, Figure 4.2).

B. ELEVATED-ELEVATED

When the atmosphere consists of two or more elevated ducts, the potential for altitudes to have extended radar ranges and areas of diminished probability of detection is increased. The extended ranges will only exist at the duct altitudes. However, the areas of radar fading may effect the radar coverage at several altitudes. Once again, the effects upon the radar coverage caused by each duct, should possibly be considered separately. From the IREPS graphical results, it appears that the more significant effects on wave propagation are caused by the duct immediately below the radar source. Locations of areas with potentially diminished radar coverage caused by the other ducts should be noted. For radar coverage displays see Appendix C, Figures C.4 and C.5 . The decision matrix constructed for an elevated duct scenario can also be used to aid the decision maker when several ducts occur simultaneously in the environment (see Chapter IV, Figure 5.3).

C. SUBREFRACTIVE-ELEVATED

When a subrefractive layer exists above an elevated duct with a separation of only 500 ft, there is a possiblity that a radar source above the two layers will experience both an area of radar fading and a bending of EM waves away from the top of this area caused by the subrefractive layer. These two anomalies, individually, contribute to a decrease in radar coverage. When considering the significance of the two refractive layers, the elevated duct appears to have a

greater effect on the radar coverage as the radiating source increases its altitude separation above the multiple layers (see Appendix C, Figure C.7).

D. ELEVATED-SUBREFRACTIVE

When the elevated duct was positioned 500 ft above the subrefractive layer, the effects of the ray bending caused by the subrefractive layer had a tendency to penetrate the radar hole. When the radar source was positioned in the duct, extended radar ranges were experienced and EM waves were bent into the area where a radar hole normally forms (see Appendix C, Figure C.9). As the radar source was positioned at increasing altitudes above the two refractive layers, EM rays were noted being directed into the radar holes yielding an improved probability of radar detection in the traditional blind spots (see Appendix C, Figures C.9 and C.10).

VII. SUMMARY

Studies of this nature on the anomalous propagation of electromagnetic waves in the atmosphere provide information that can potentially be used by airborne early warning and reconnaissance aircraft in gaining tactical advantage against an adversary. This study has concentrated its effort on a tactical analysis concerning the effects of subrefractive layers, elevated ducts, and multiple layers on both radiating and non-radiating aircraft. An initial analysis of the subrefractive layers and elevated duct scenarios via the IREPS model revealed the location of areas of diminished probability of detection that may be experienced by these aircraft. It was noted that if a radar source was positioned below a refractive layer, no anomalous effects were encountered by the aircraft. Likewise, the greater the altitude separation above the refractive layers, the less consequence of the anomalies. Extended ranges of radar reception and coverage were experienced when the radar source was positioned in the duct; however, these effects only applied to the altitude of the duct. It was noted that the IREPS model does not consider radar reflections off the surface of the earth in calculating the results. The radar reflections may improve the detection coverage in some of the scenarios.

This study, based upon the interpretation of IREPS, provides only a qualitative analysis of a search radar's performance. However, this type of analysis can be used as a basis for evaluation of the relative capabilities of reconnaissance and early warning aircraft for each given scenario. Additional trials can be simulated using the actual radar parameters of a specific radar source of

interest. From these results a decision matrix and graphical decision tools can be constructed which may assist in tactical planning. Further analysis involving actual test flights under similar environmental conditions will provide added information about the effects of subrefractive layers and elevated ducts on aircraft radars.

APPENDIX A

SUBREFRACTIVE LAYERS EXAMPLES

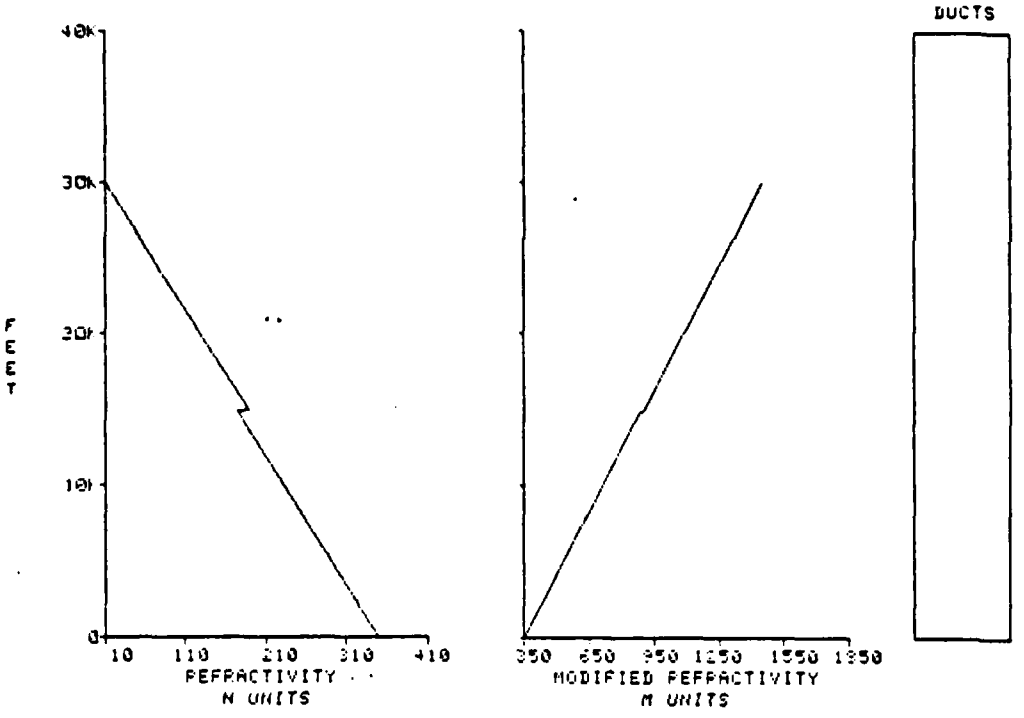

LEVEL	FEET	N UNITS	N/Kft	M UNITS	CONDITION
1	0.0	350.0	-11.8	350.0	NORMAL
2	14,800.0	175.4	60.0	883.4	SUB
3	15,000.0	187.4	-11.8	905.0	NORMAL
4	30,000.0	10.4	------	1,445.6	------

Figure A.1 Subrefractive Layer Profile: +60 N units/kft, 15,000 ft.

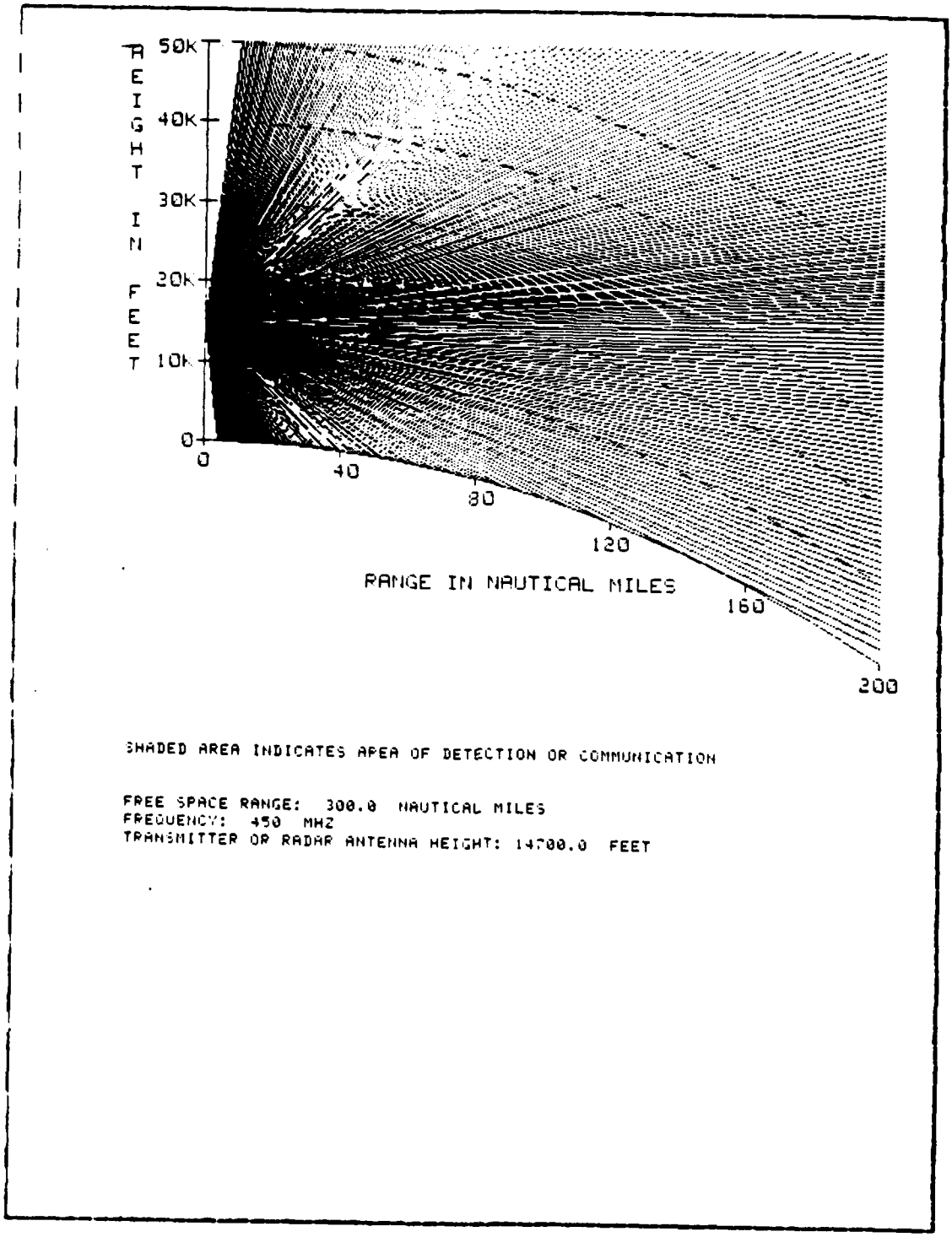

Figure A.2 Sub: +60 N units/kft, 15,000 ft. Radar Alt. 14,700 ft.

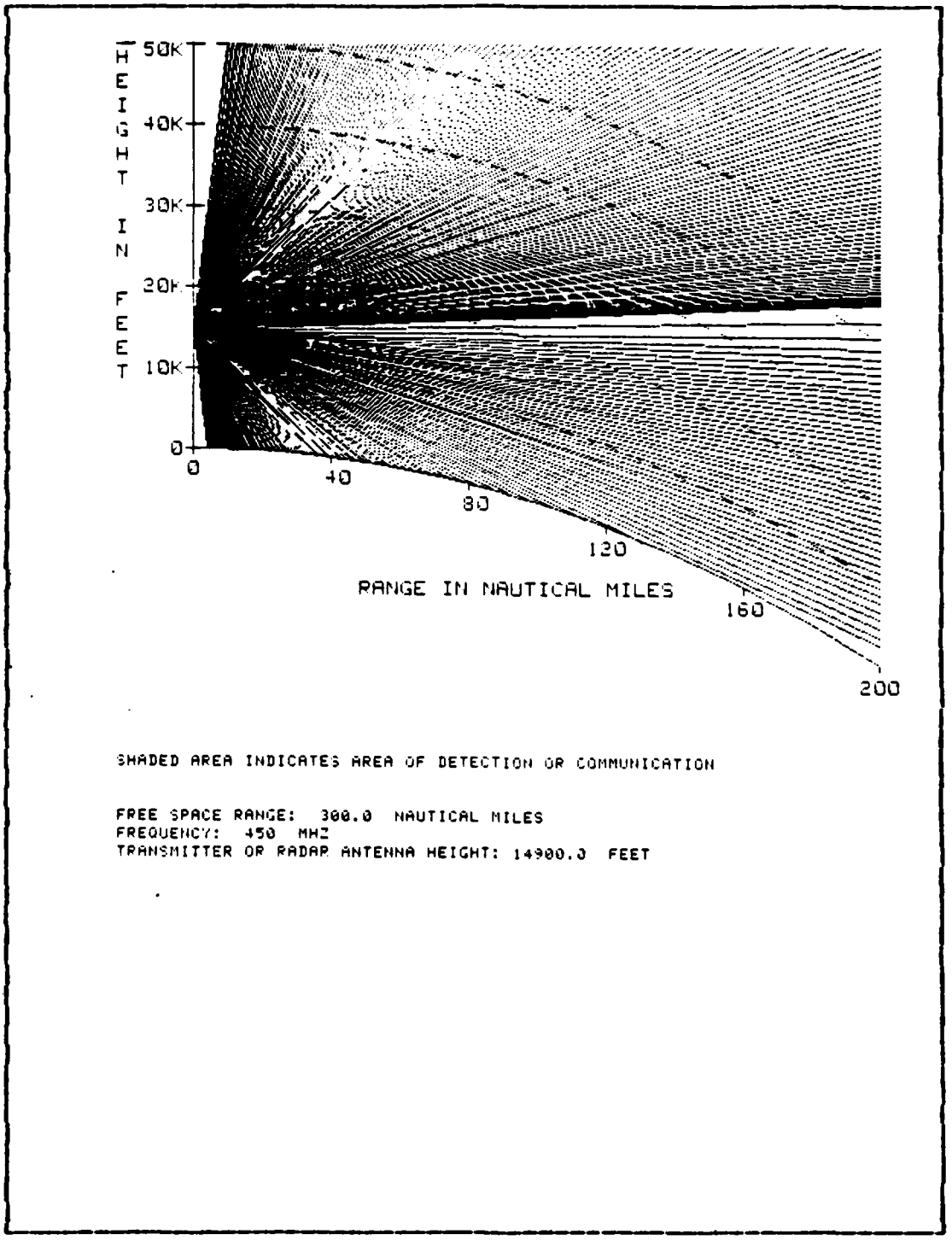

Figure A.3 Sub: +60 N units/kft, 15,000 ft. Radar Alt. 14,900 ft.

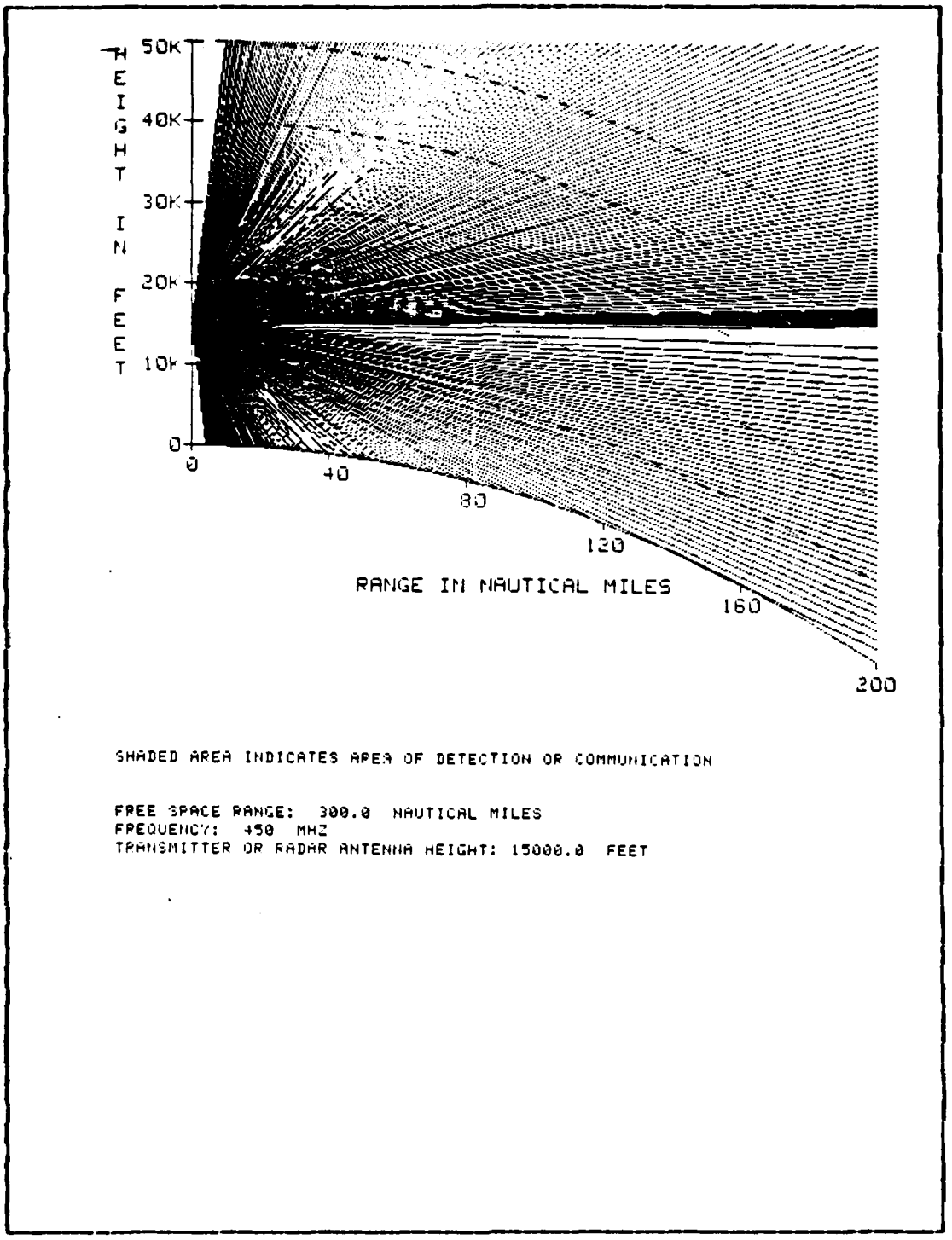

Figure A.4 Sub: +60 N units/kft, 15,000 ft. Radar Alt. 15,000 ft.

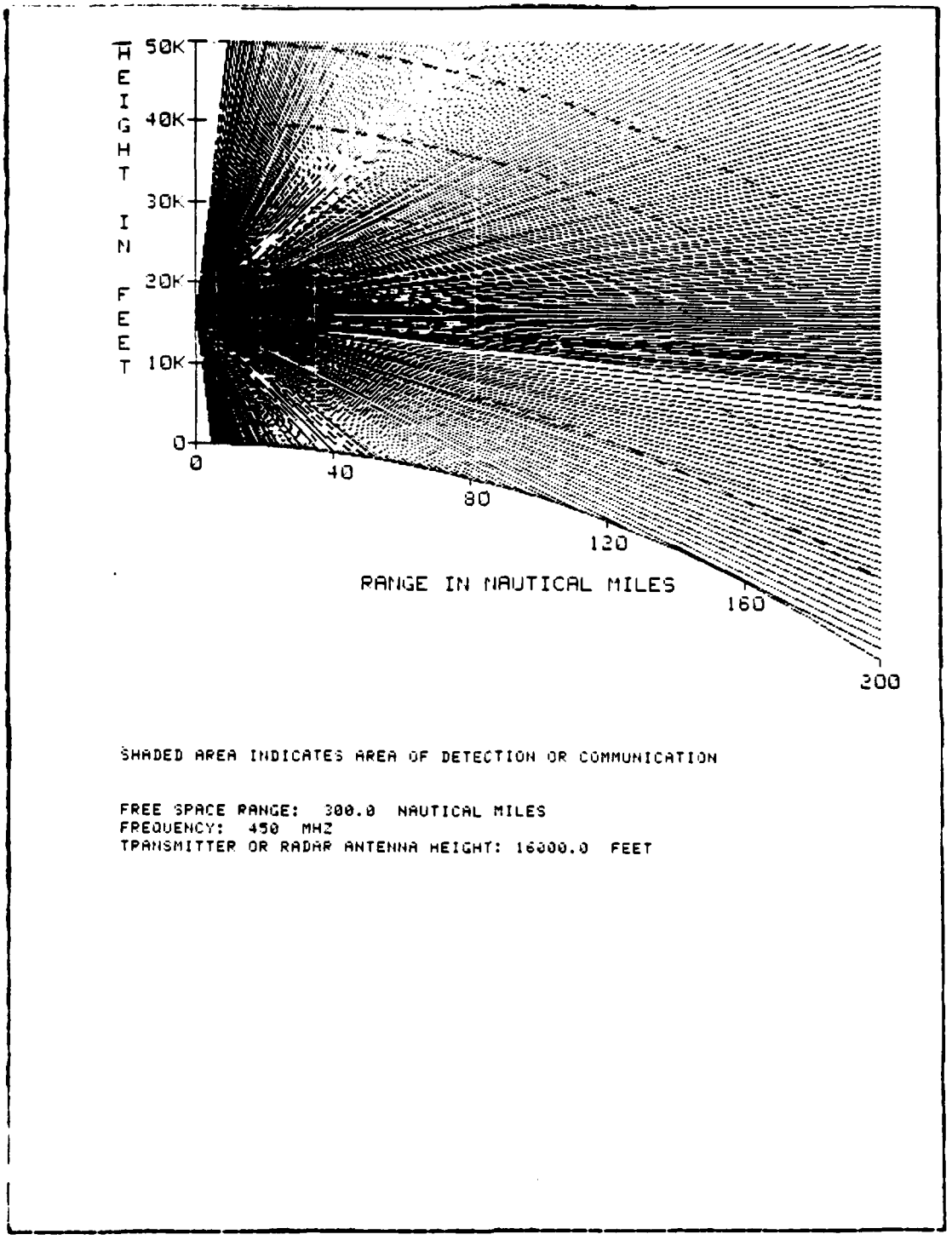

Figure A.5 Sub: +60 N units/kft, 15,000 ft. Radar Alt. 16,000 ft.

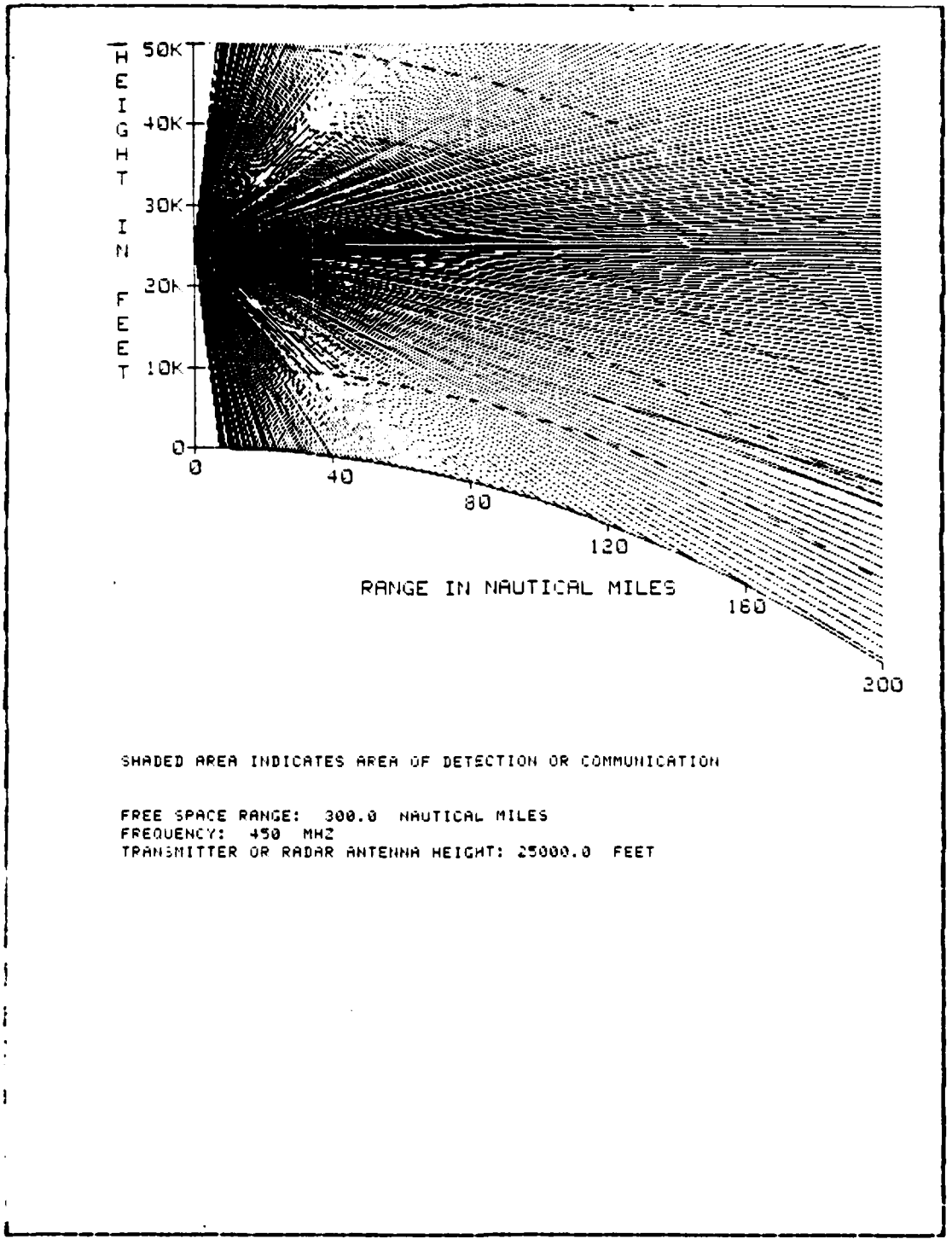

Figure A.6 Sub: +60 N units/kft, 15,000 ft. Radar Alt. 25,000 ft.

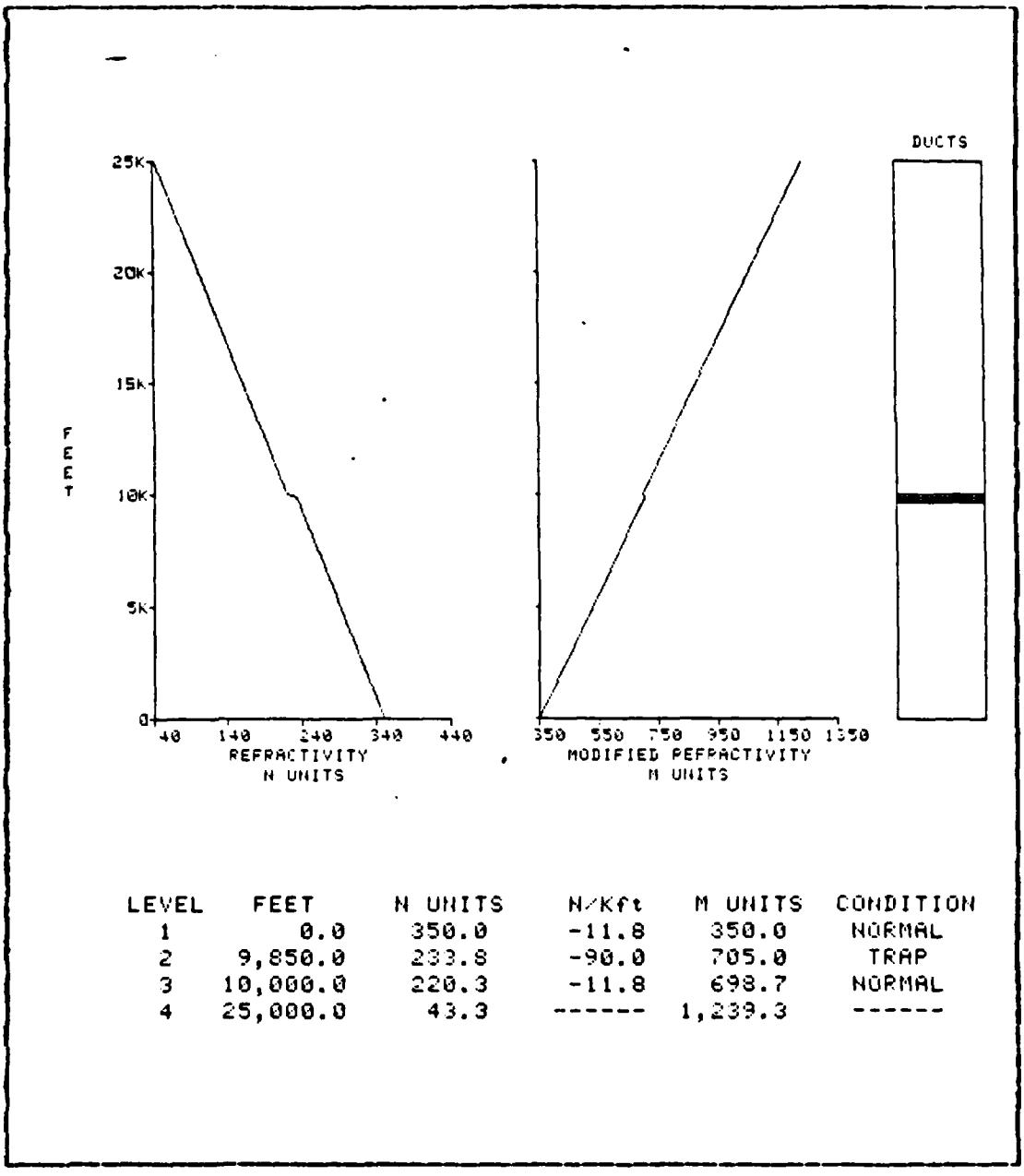

LEVEL	FEET	N UNITS	N/Kft	M UNITS	CONDITION
1	0.0	350.0	-11.8	350.0	NORMAL
2	9,850.0	233.8	-90.0	705.0	TRAP
3	10,000.0	220.3	-11.8	698.7	NORMAL
4	25,000.0	43.3	------	1,239.3	------

Figure B.1 Elevated Layer Profile: -90 N units/kft, 10,000 ft.

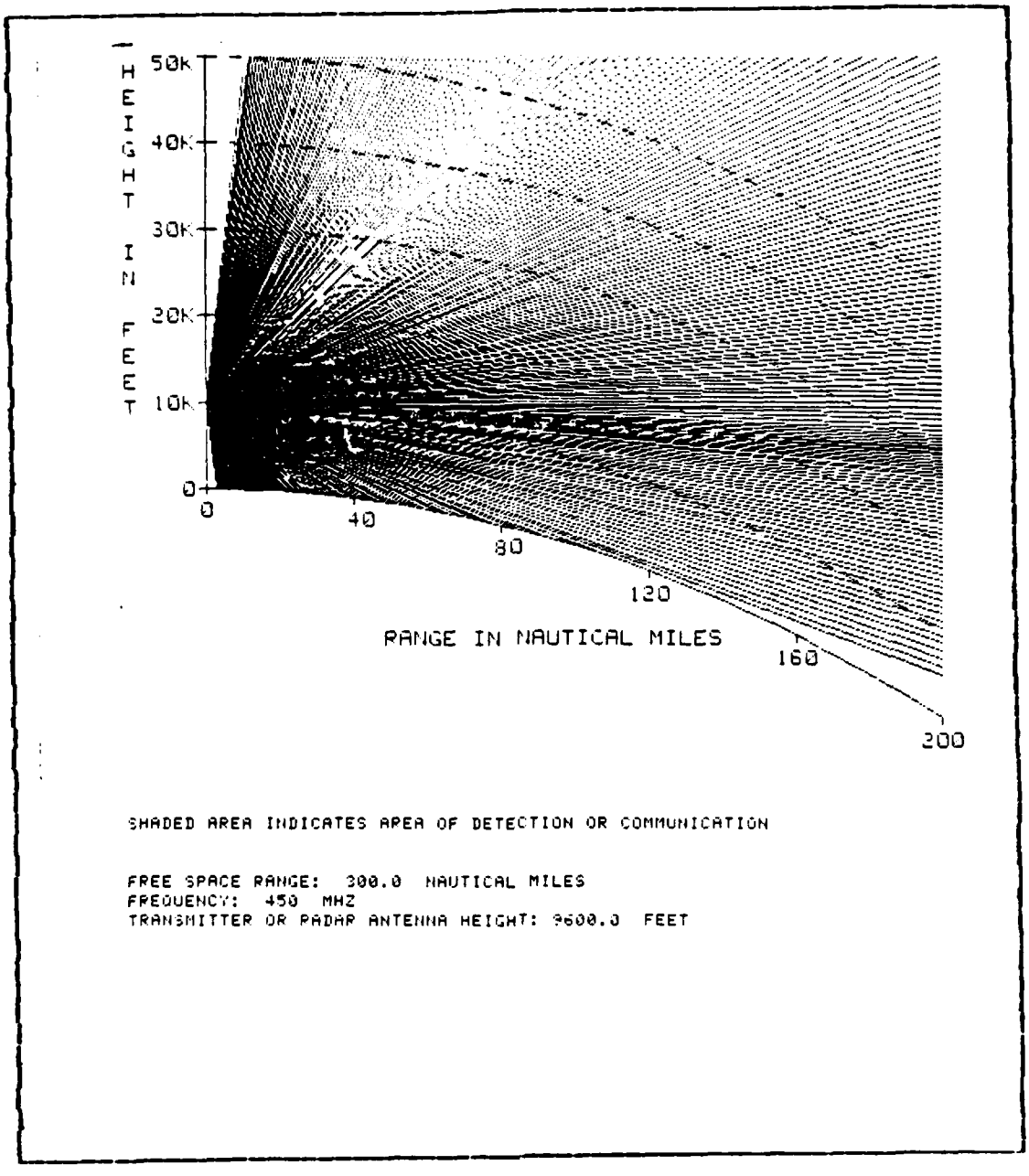

Figure B.2 **Elev: -90 N units/kft, 10,000 ft. Radar Alt. 9,600 ft.**

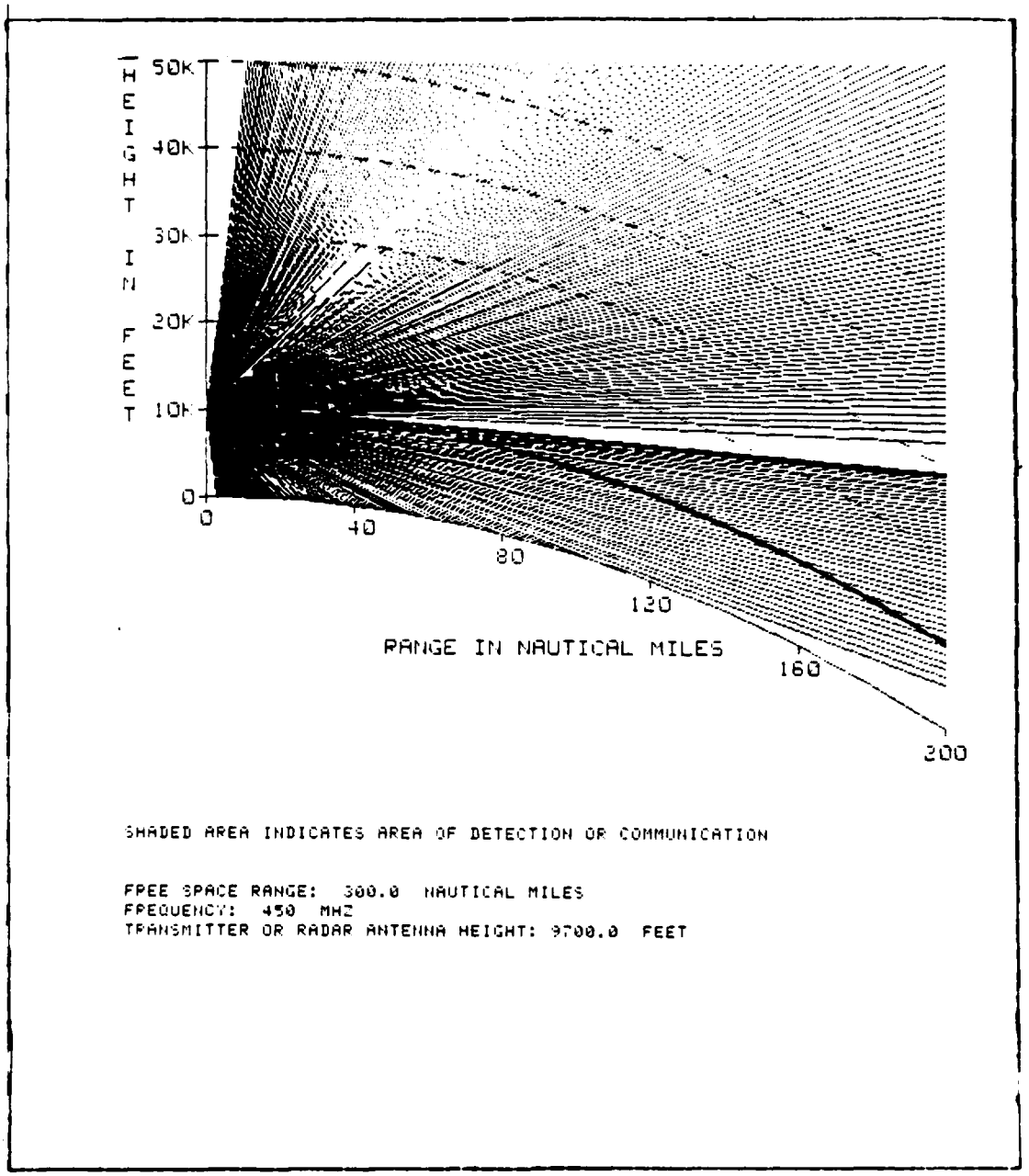

Figure B.3 Elev: -90 N units/kft, 10,000 ft. Radar Atl. 9,700 ft.

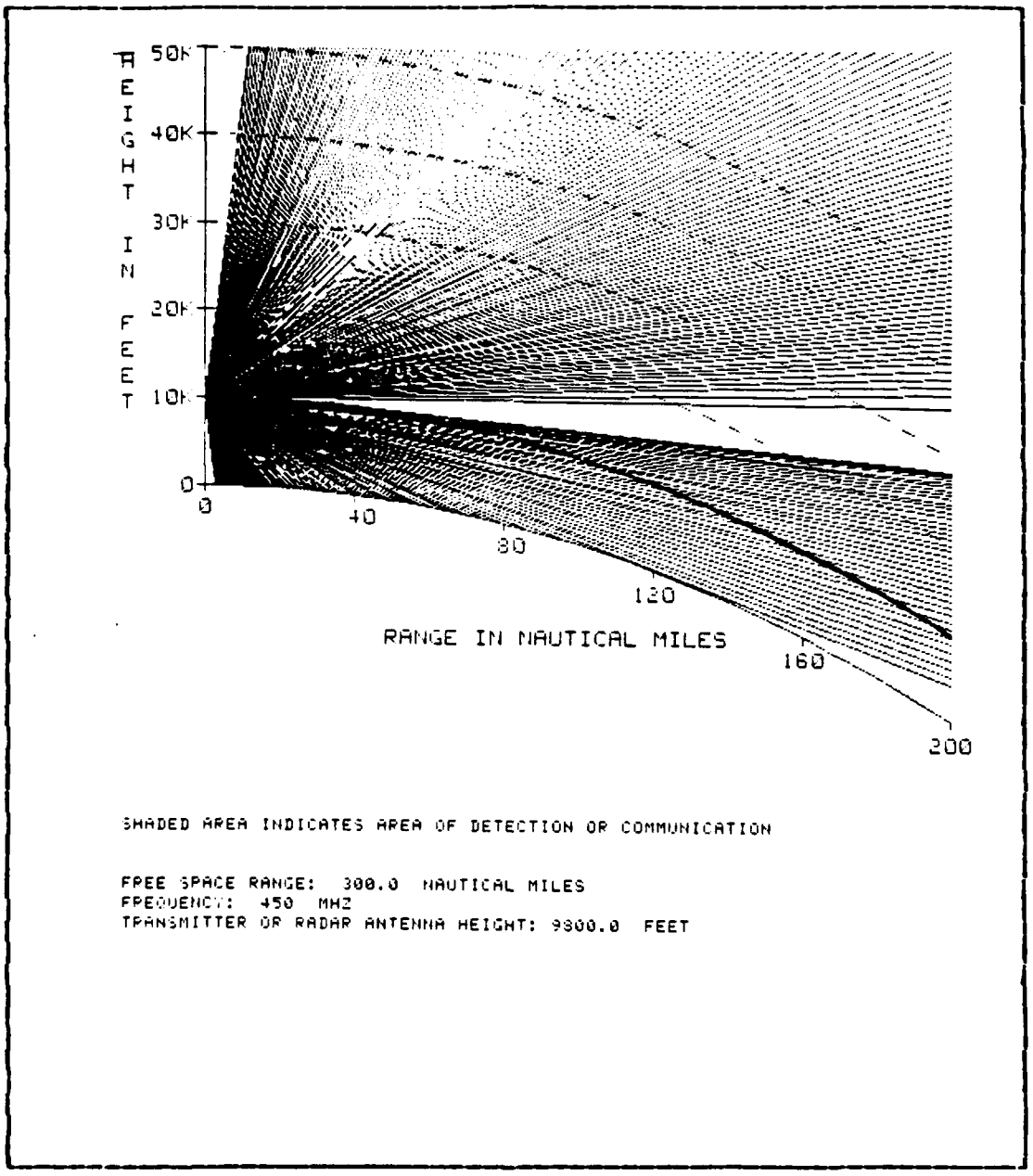

Figure B.4 **Elev: -90 N units/kft, 10,000 ft. Radar Alt. 9,800 ft.**

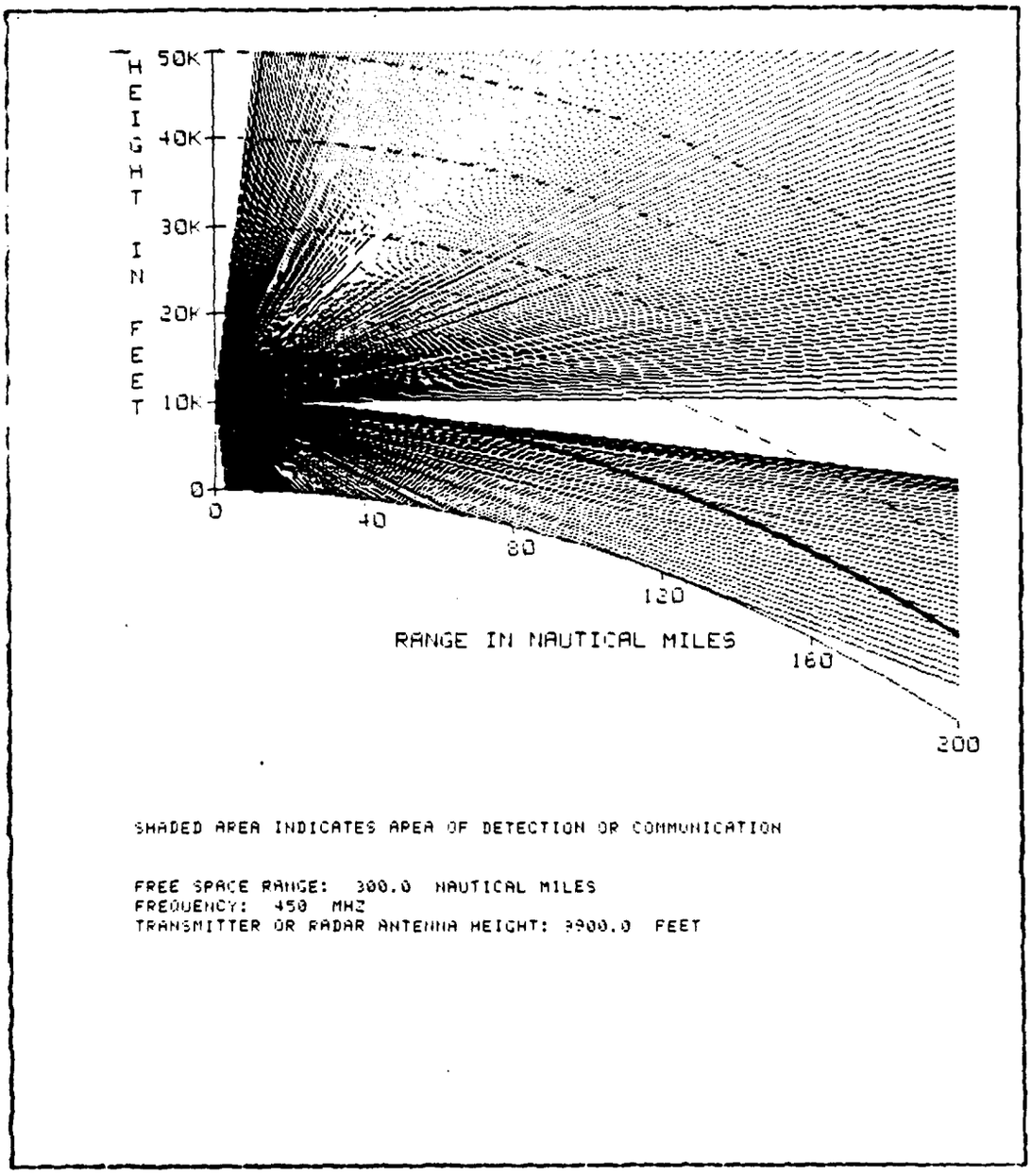

Figure B.5 **Elev: -90 N units/kft, 10,000 ft. Radar Alt. 9,900 ft.**

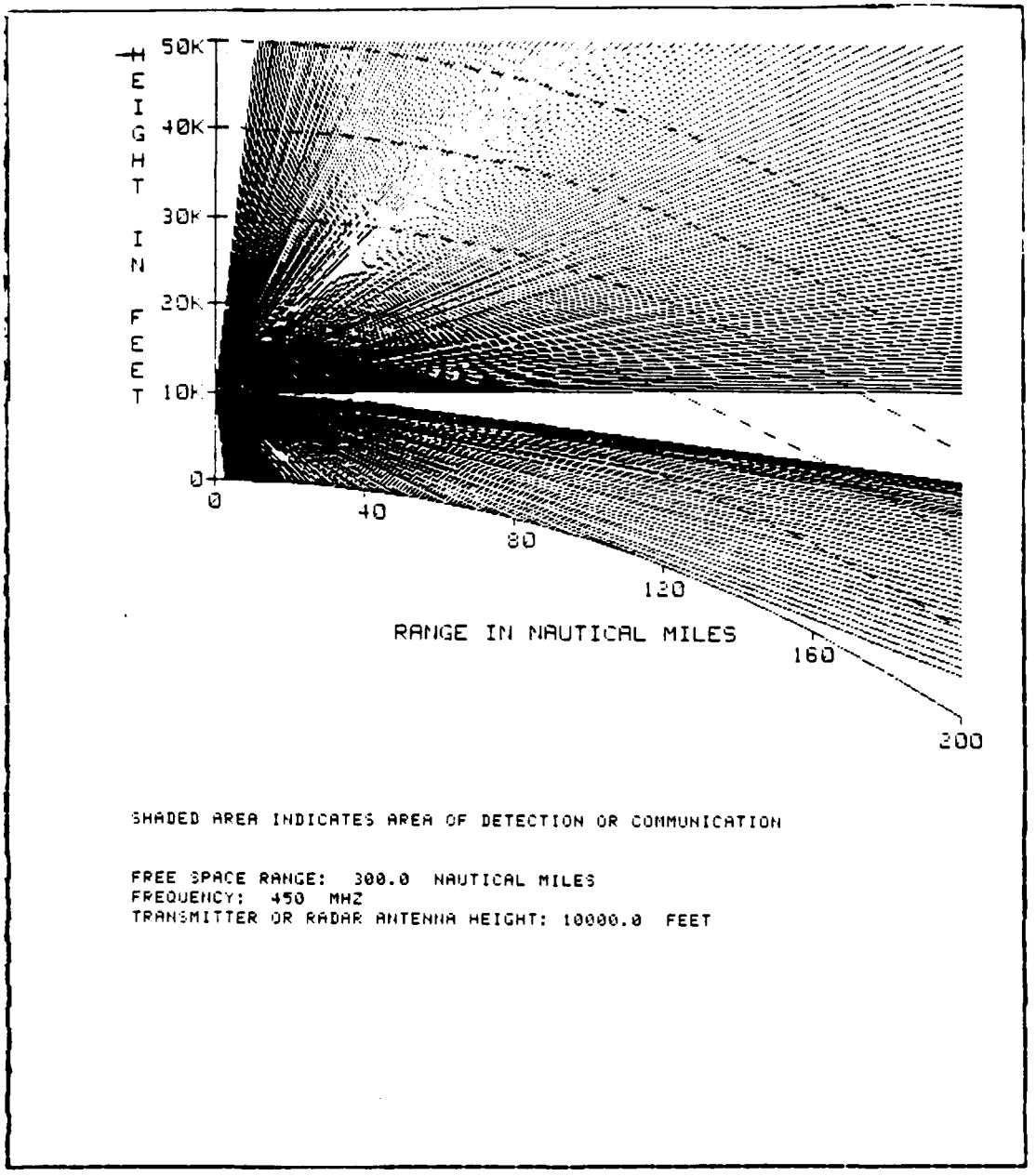

Figure B.6 Elev: -90 N units/kft, 10,000 ft. Radar Alt. 10,000 ft.

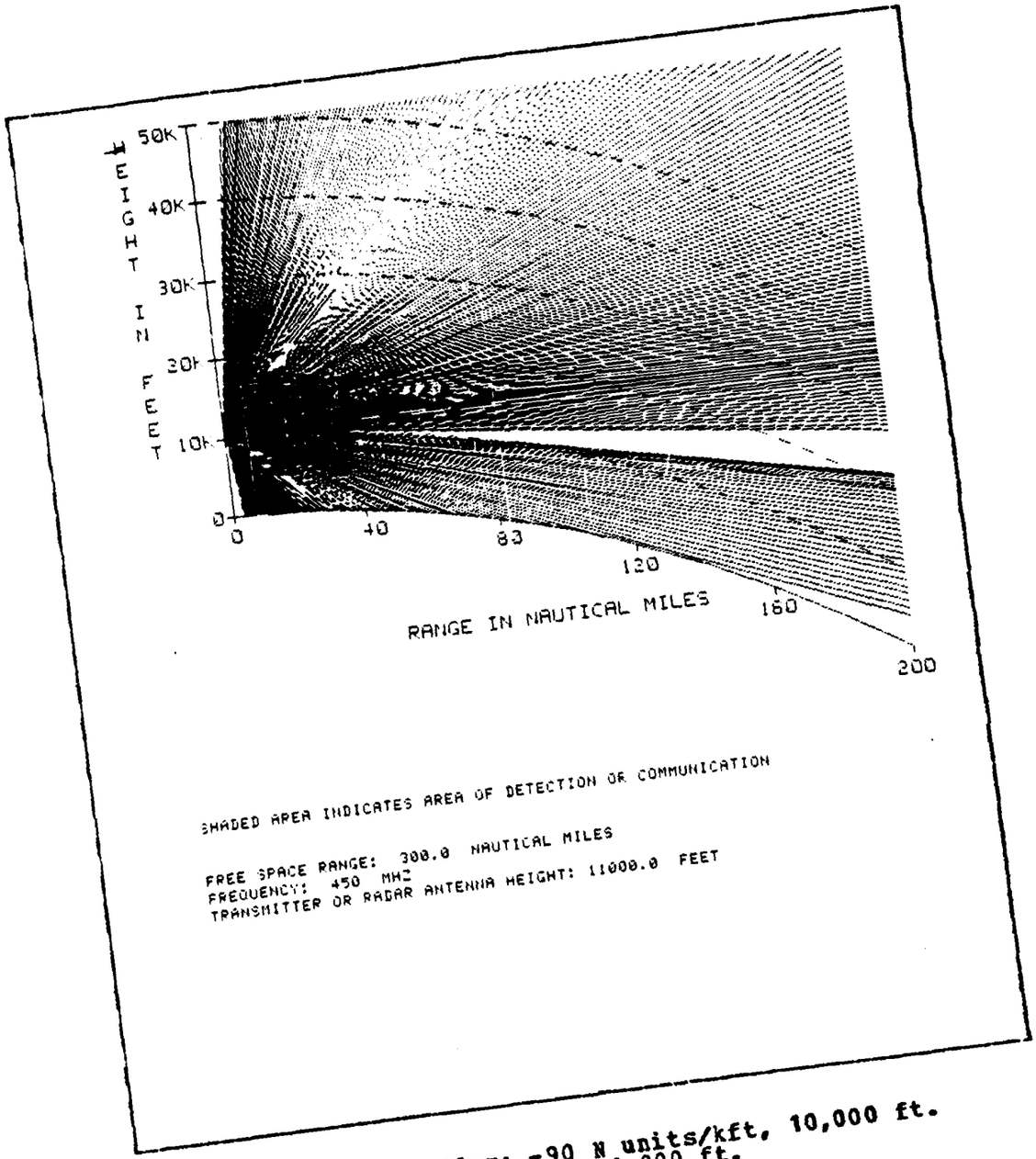

Figure B.7 Elev: -90 N units/kft, 10,000 ft. Radar Alt. 11,000 ft.

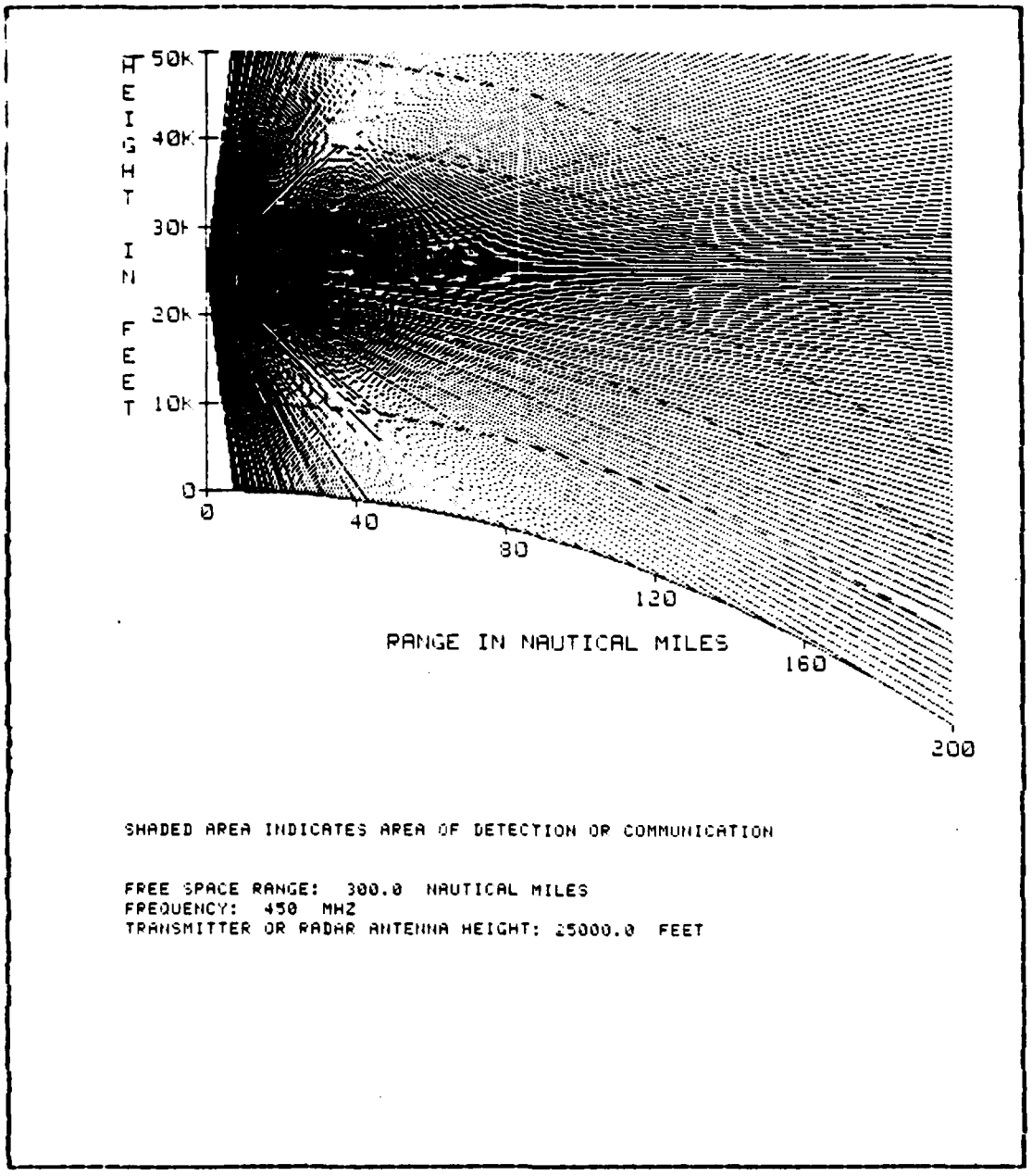

Figure B.8 Elev: -90 N units/kft, 10,000 ft. Radar Alt. 25,000 ft.

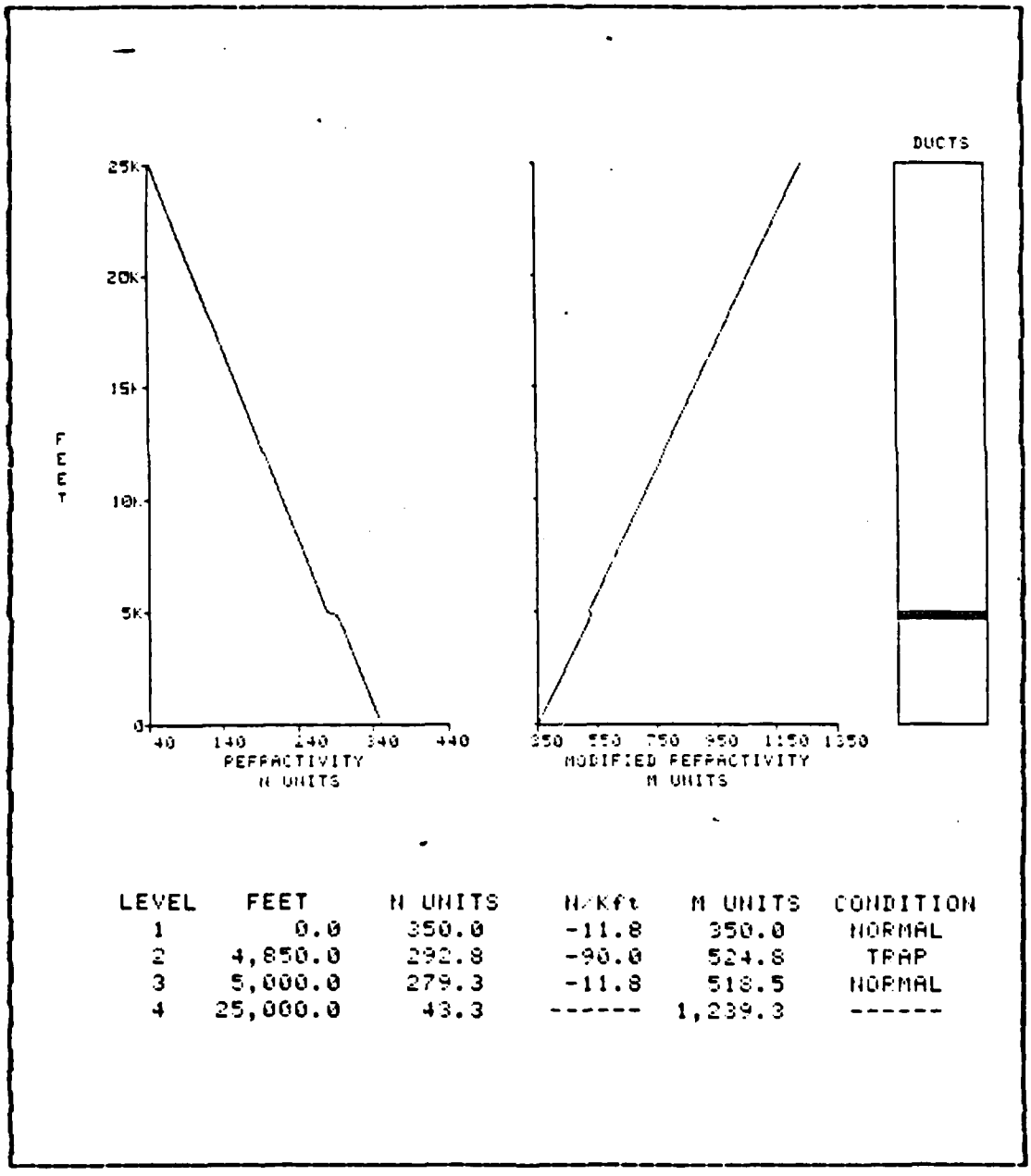

LEVEL	FEET	N UNITS	N/Kft	M UNITS	CONDITION
1	0.0	350.0	-11.8	350.0	NORMAL
2	4,850.0	292.8	-90.0	524.8	TRAP
3	5,000.0	279.3	-11.8	518.5	NORMAL
4	25,000.0	43.3	------	1,239.3	------

Figure B.9 Elevated Layer Profile: -90 N units/kft, 5,000 ft.

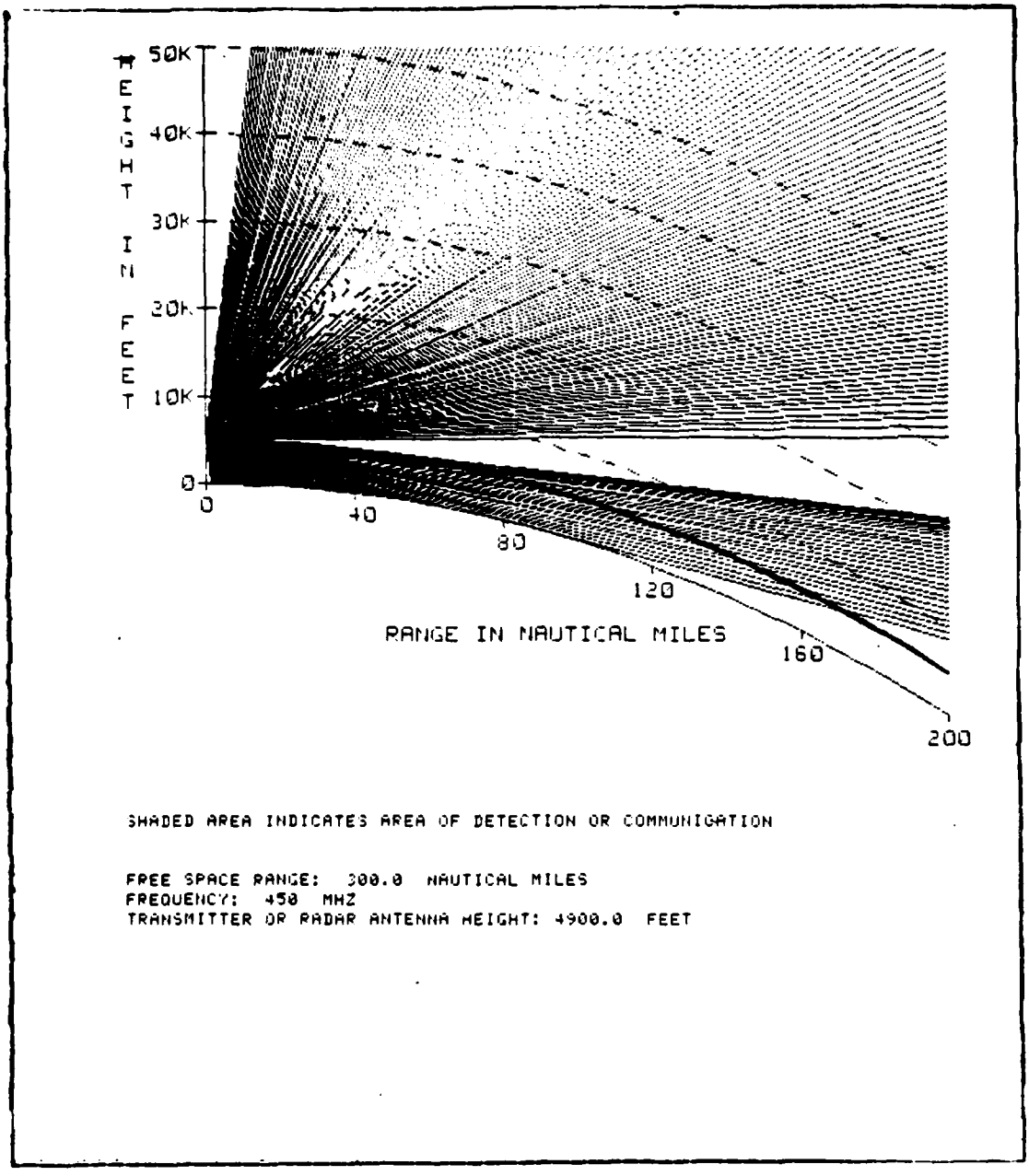

Figure B.10 Elev: -90 N units/kft, 5,000 ft. Radar Alt. 4,900 ft.

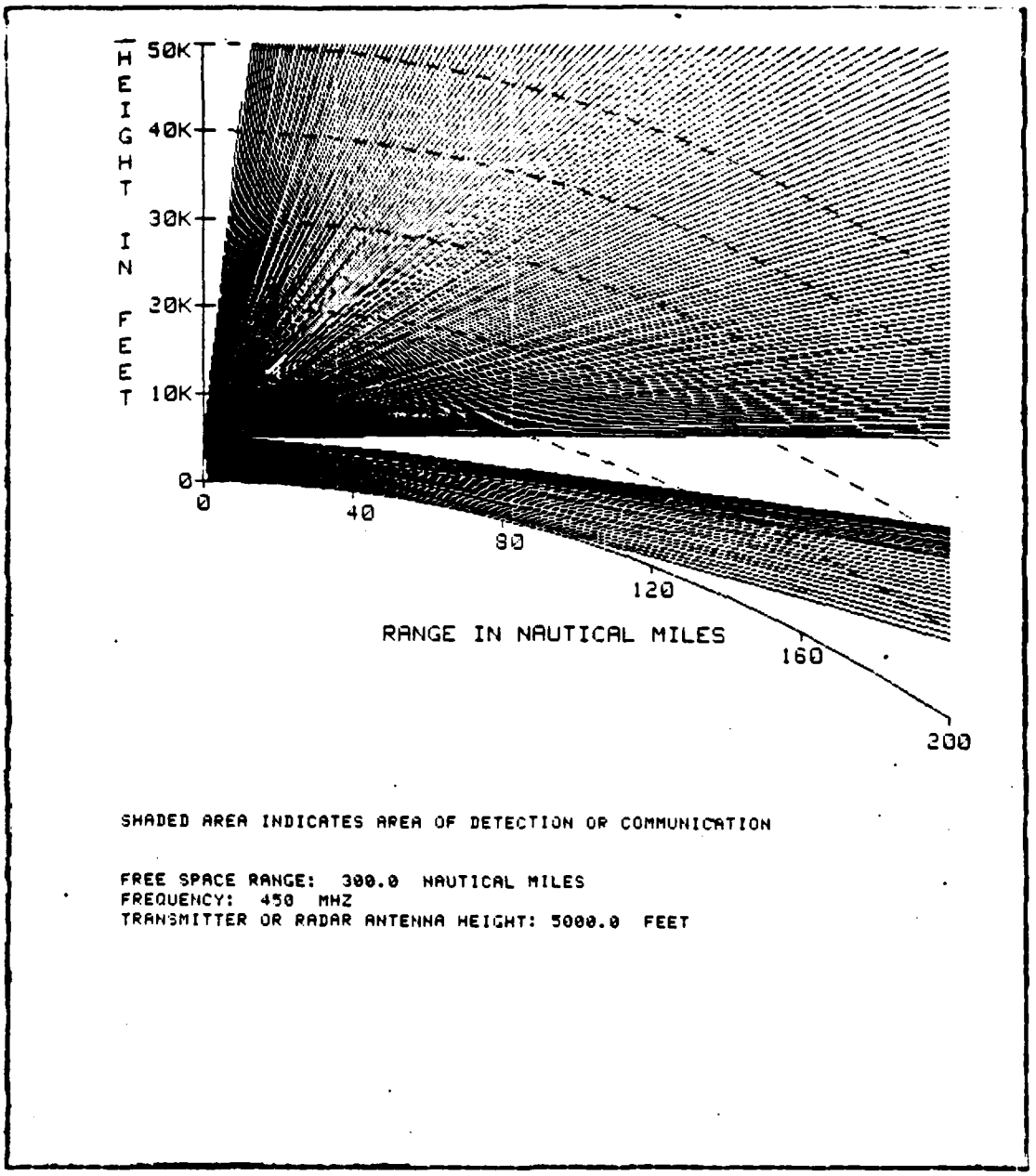

Figure B.11 Elev: -90 N units/kft, 5,000 ft. Radar Alt. 5,000 ft.

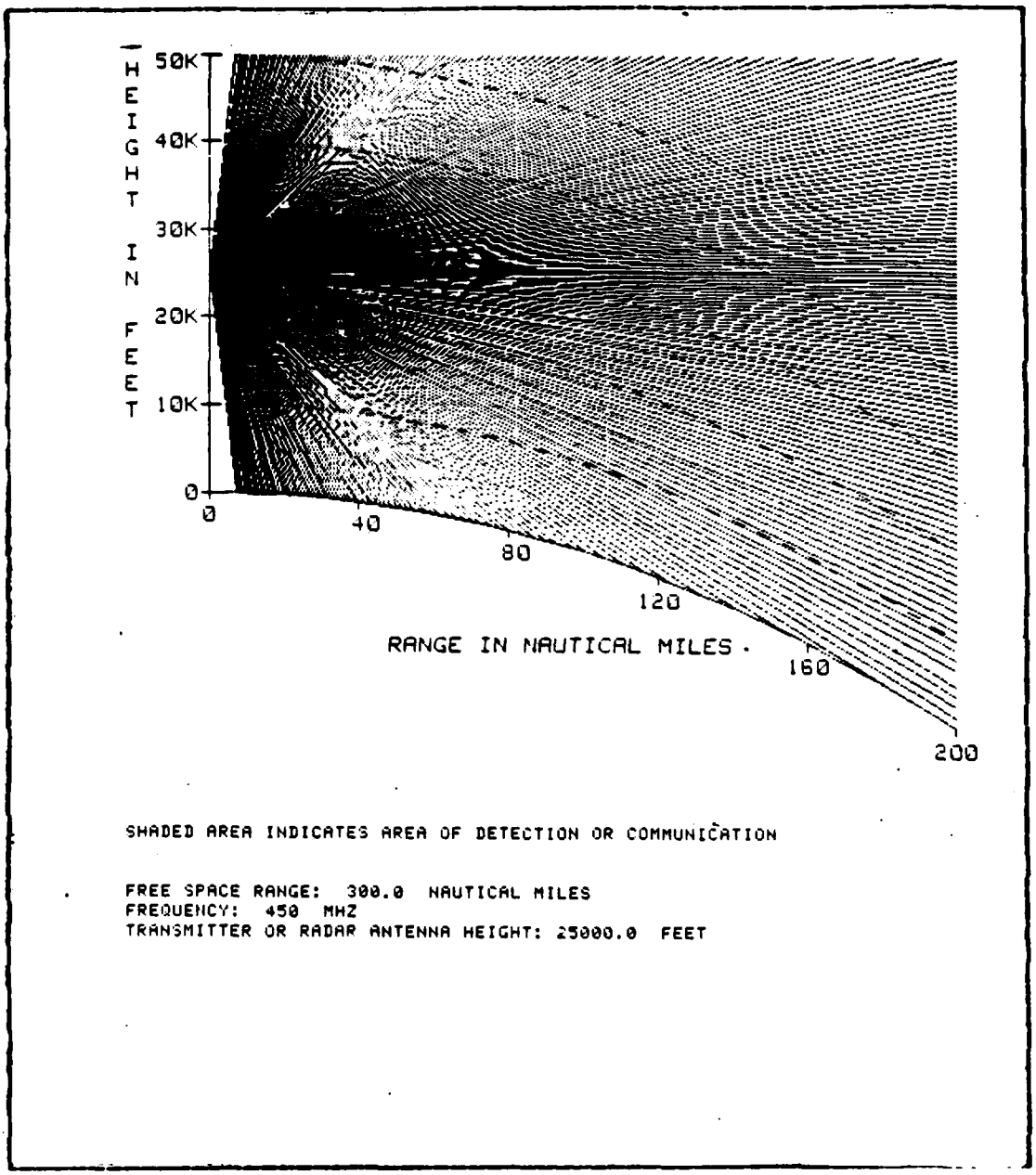

Figure B.12 Elev: -90 N units/kft, 5,000 ft Radar Alt. 25,000 ft.

APPENDIX C
MULTIPLE LAYERS EXAMPLES

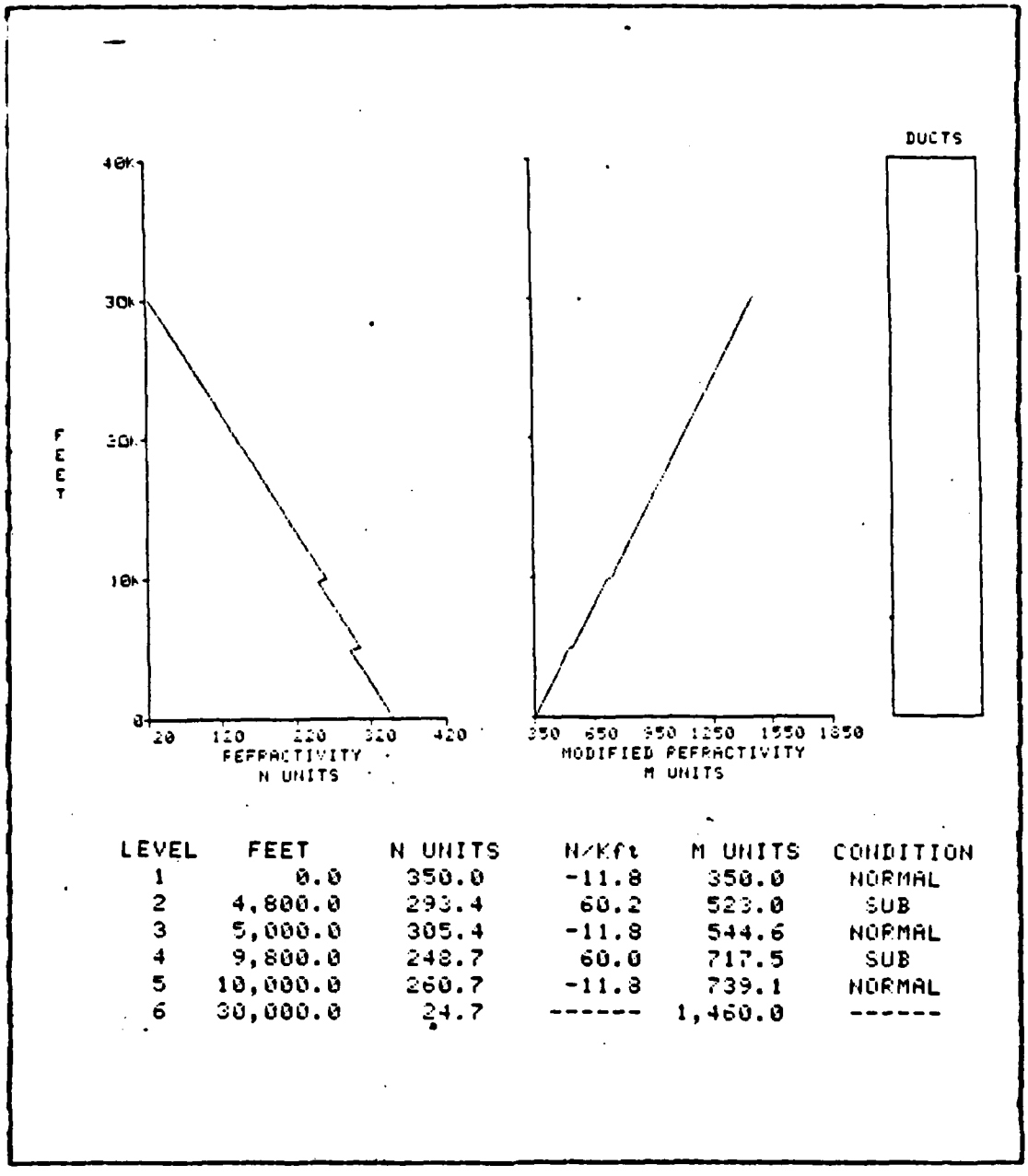

LEVEL	FEET	N UNITS	N/Kft	M UNITS	CONDITION
1	0.0	350.0	-11.8	350.0	NORMAL
2	4,800.0	293.4	60.2	523.0	SUB
3	5,000.0	305.4	-11.8	544.6	NORMAL
4	9,800.0	248.7	60.0	717.5	SUB
5	10,000.0	260.7	-11.8	739.1	NORMAL
6	30,000.0	24.7	------	1,460.0	------

Figure C.1 Sub/Sub Profile: +60 N units/kft, 10 kft/5 kft.

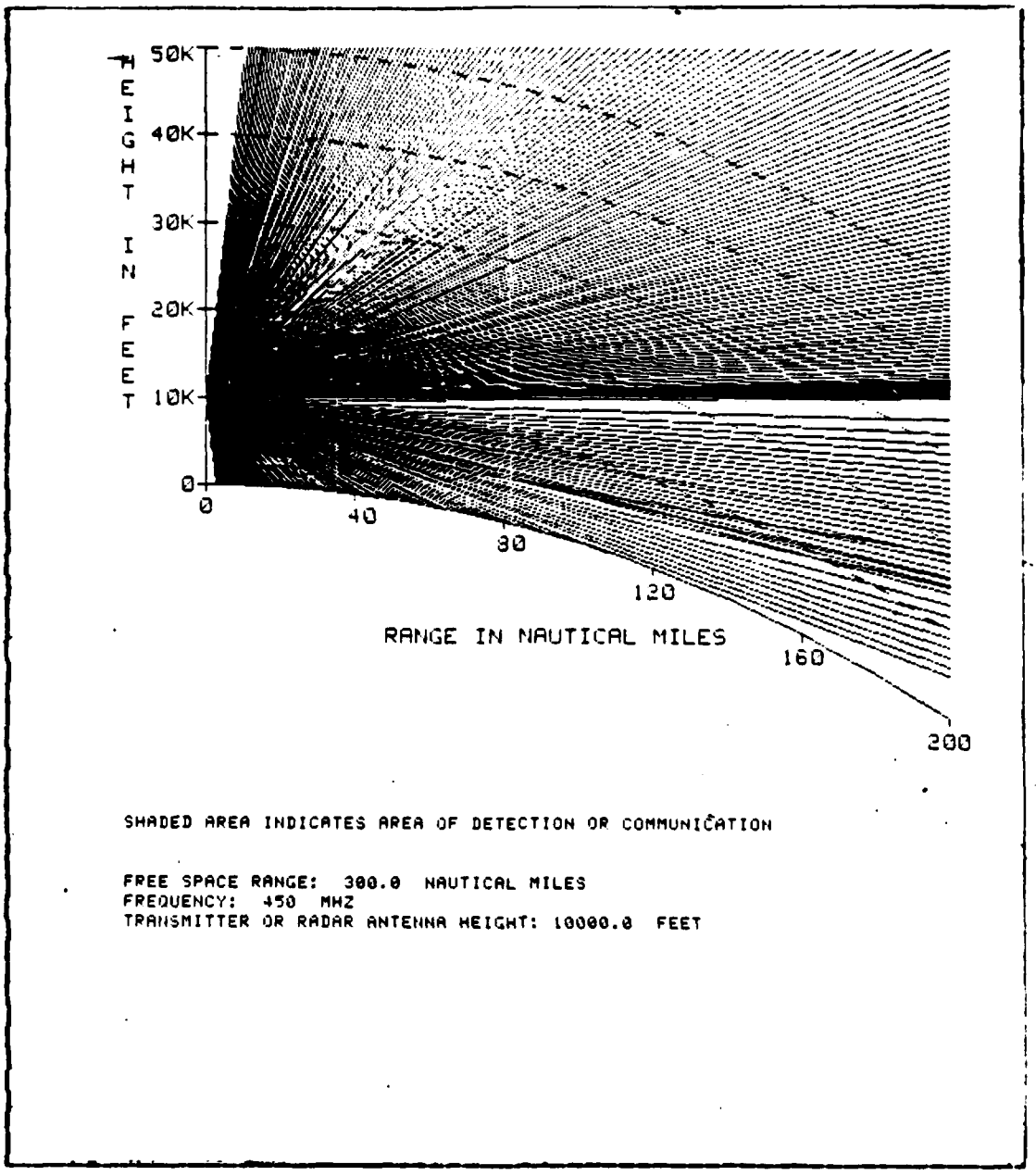

Figure C.2 Sub/Sub: +60 N units/kft, 10 kft/5 kft. Radar Alt. 10,000 ft.

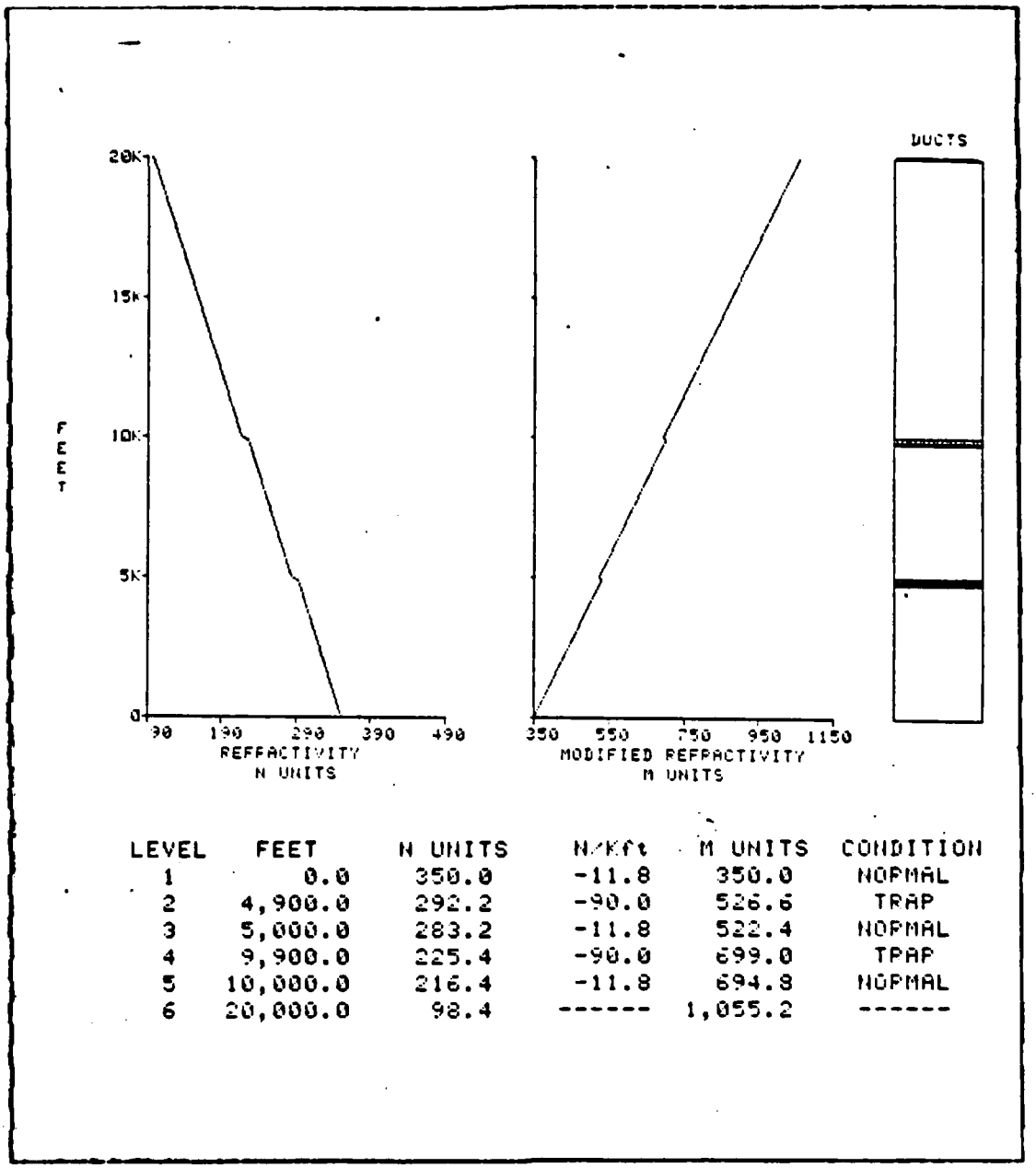

LEVEL	FEET	N UNITS	N/Kft	M UNITS	CONDITION
1	0.0	350.0	-11.8	350.0	NORMAL
2	4,900.0	292.2	-90.0	526.6	TRAP
3	5,000.0	283.2	-11.8	522.4	NORMAL
4	9,900.0	225.4	-90.0	699.0	TRAP
5	10,000.0	216.4	-11.8	694.8	NORMAL
6	20,000.0	98.4	------	1,055.2	------

Figure C.3 Elev/Elev Profile: -90 N units/kft, 10 kft/5 kft.

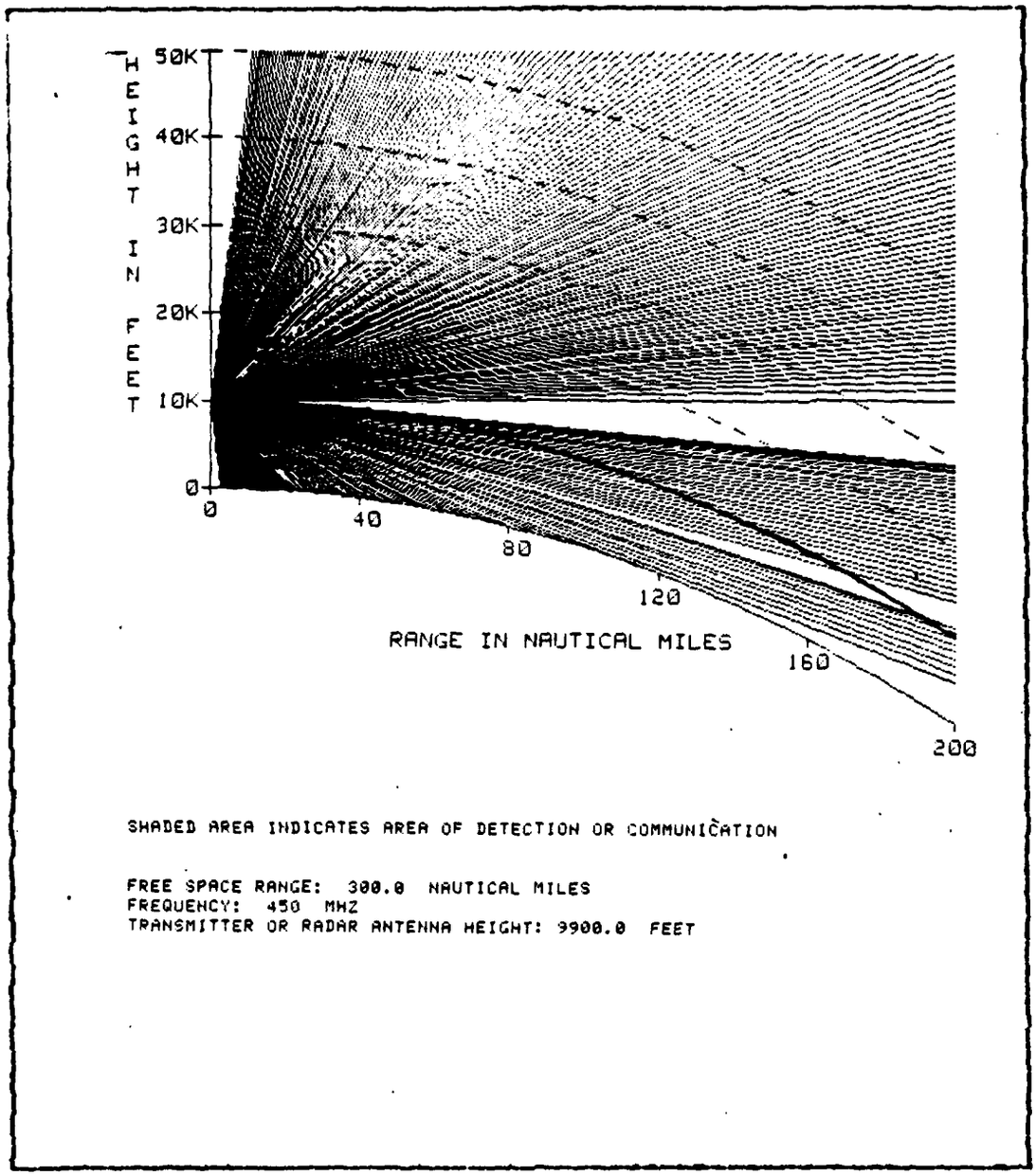

Figure C.4 Elev/Elev: -90 N units/kft, 10 kft/5 kft. Radar Alt. 9,900 ft.

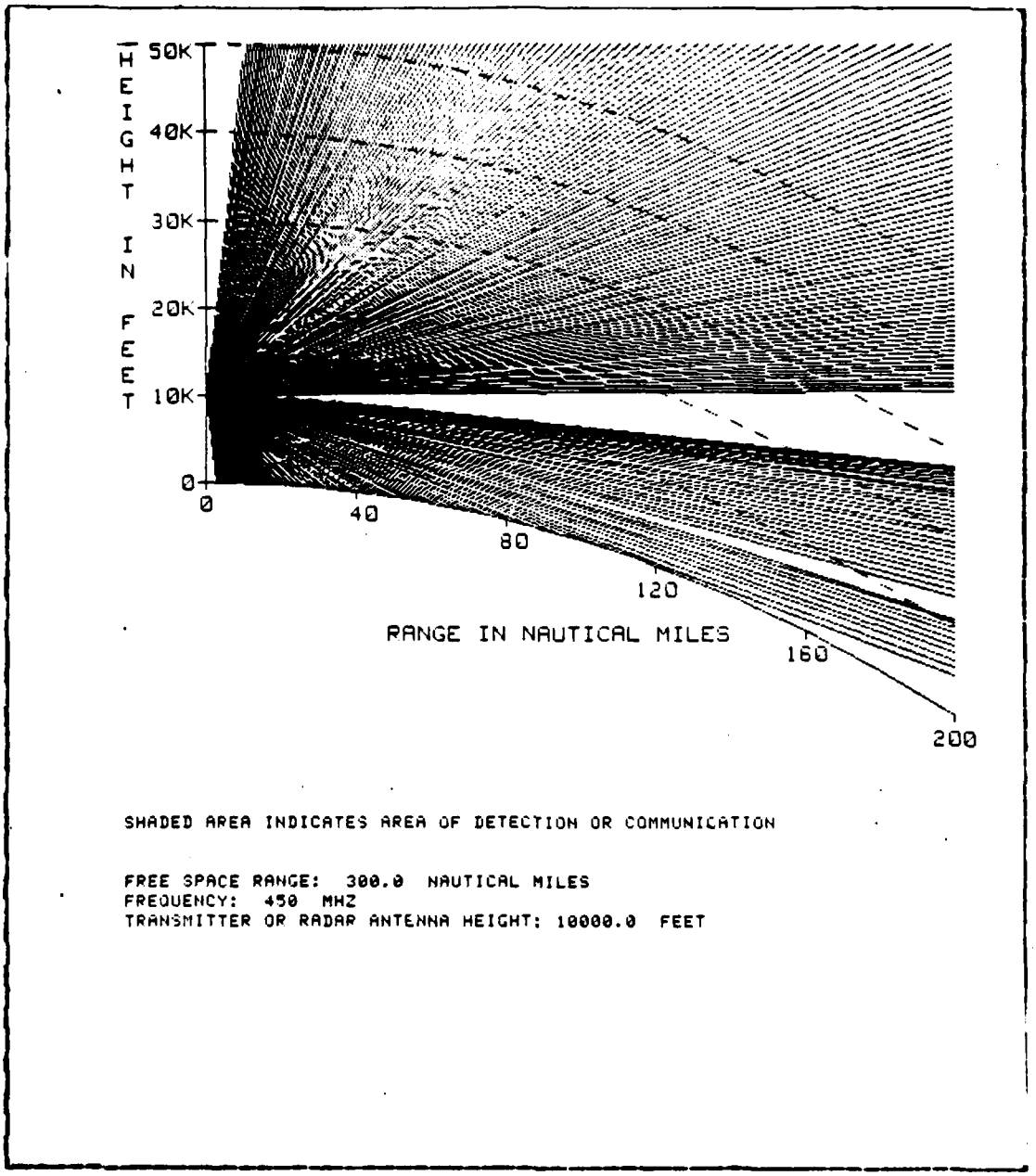

Figure C.5 Elev/Elev: -90 N units/kft, 10 kft/5 kft. Radar Alt. 10,000 ft.

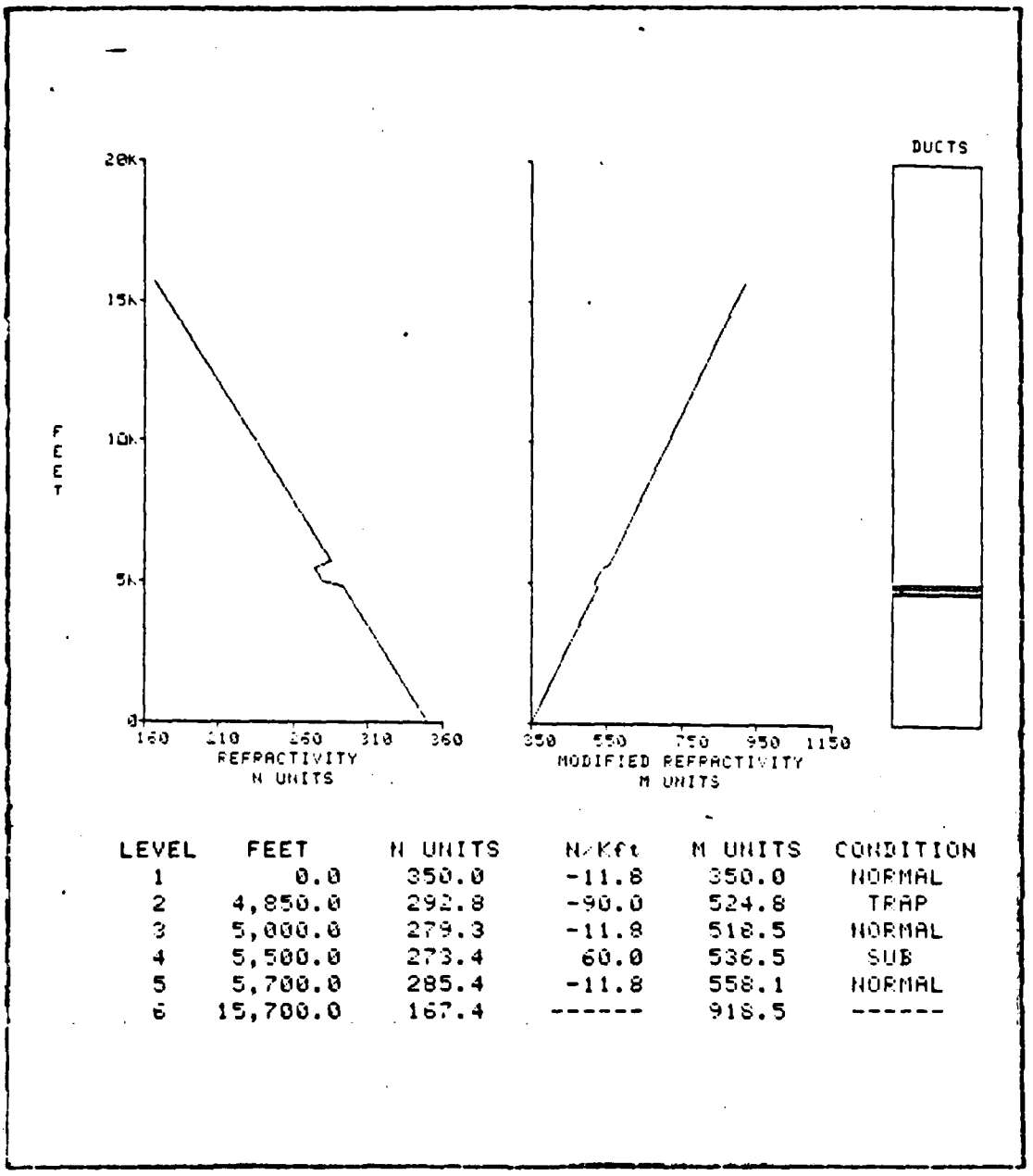

LEVEL	FEET	N UNITS	N/Kft	M UNITS	CONDITION
1	0.0	350.0	-11.8	350.0	NORMAL
2	4,850.0	292.8	-90.0	524.8	TRAP
3	5,000.0	279.3	-11.8	518.5	NORMAL
4	5,500.0	273.4	60.0	536.5	SUB
5	5,700.0	285.4	-11.8	558.1	NORMAL
6	15,700.0	167.4	------	918.5	------

Figure C.6 Sub/Elev Profile: +60/-90 N units/kft, 5.5 kft/5 kft.

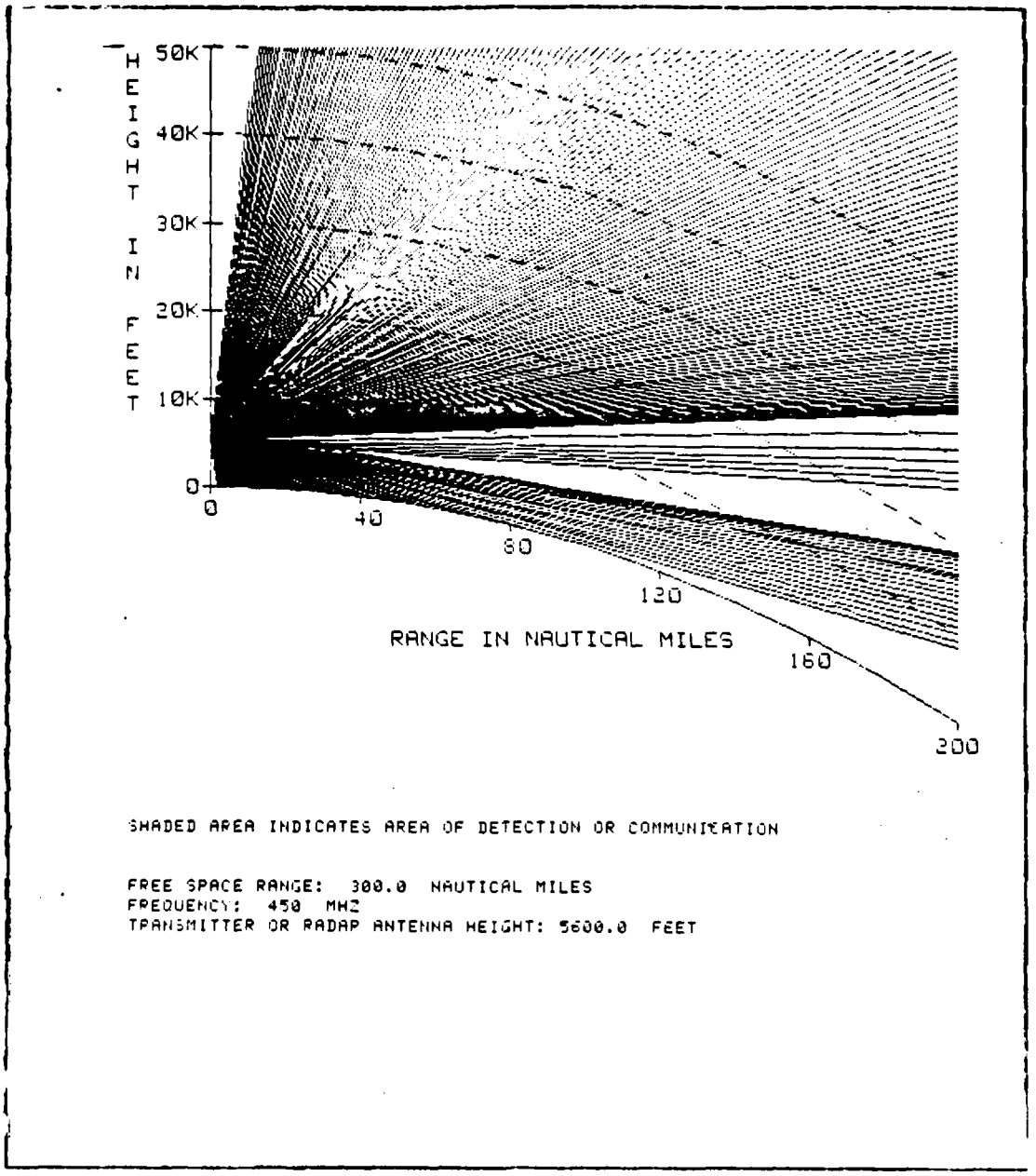

Figure C.7 Sub/Elev: +60/-90 N units/kft, 5.5 kft/5kft Radar Alt. 5,600 ft.

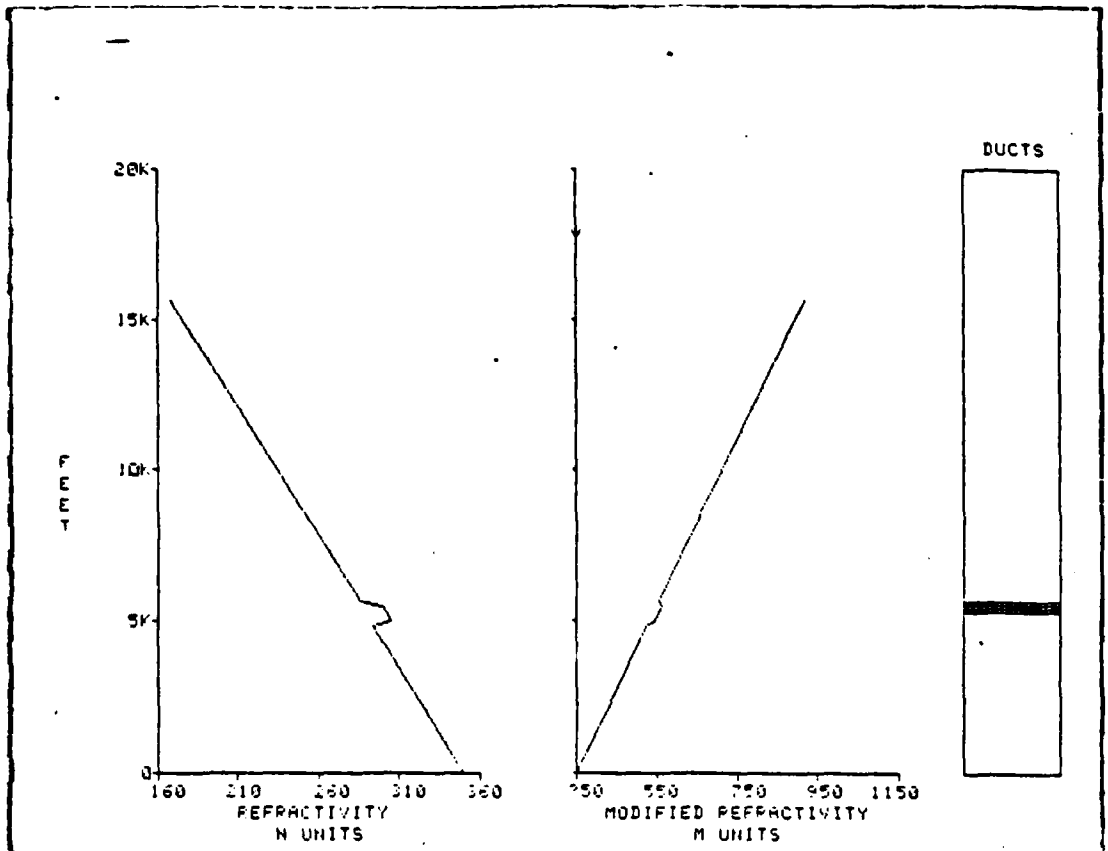

LEVEL	FEET	N UNITS	N/Kft	M UNITS	CONDITION
1	0.0	350.0	-11.8	350.0	NORMAL
2	4,800.0	293.4	60.0	523.0	SUB
3	5,000.0	305.4	-11.8	544.6	NORMAL
4	5,500.0	299.5	-90.0	562.6	TRAP
5	5,650.0	286.0	-11.8	556.3	NORMAL
6	15,650.0	168.0	------	916.7	------

Figure C.8 Elev/Sub Profile: -90/+60 N units/kft, 5.5 kft/5 kft.

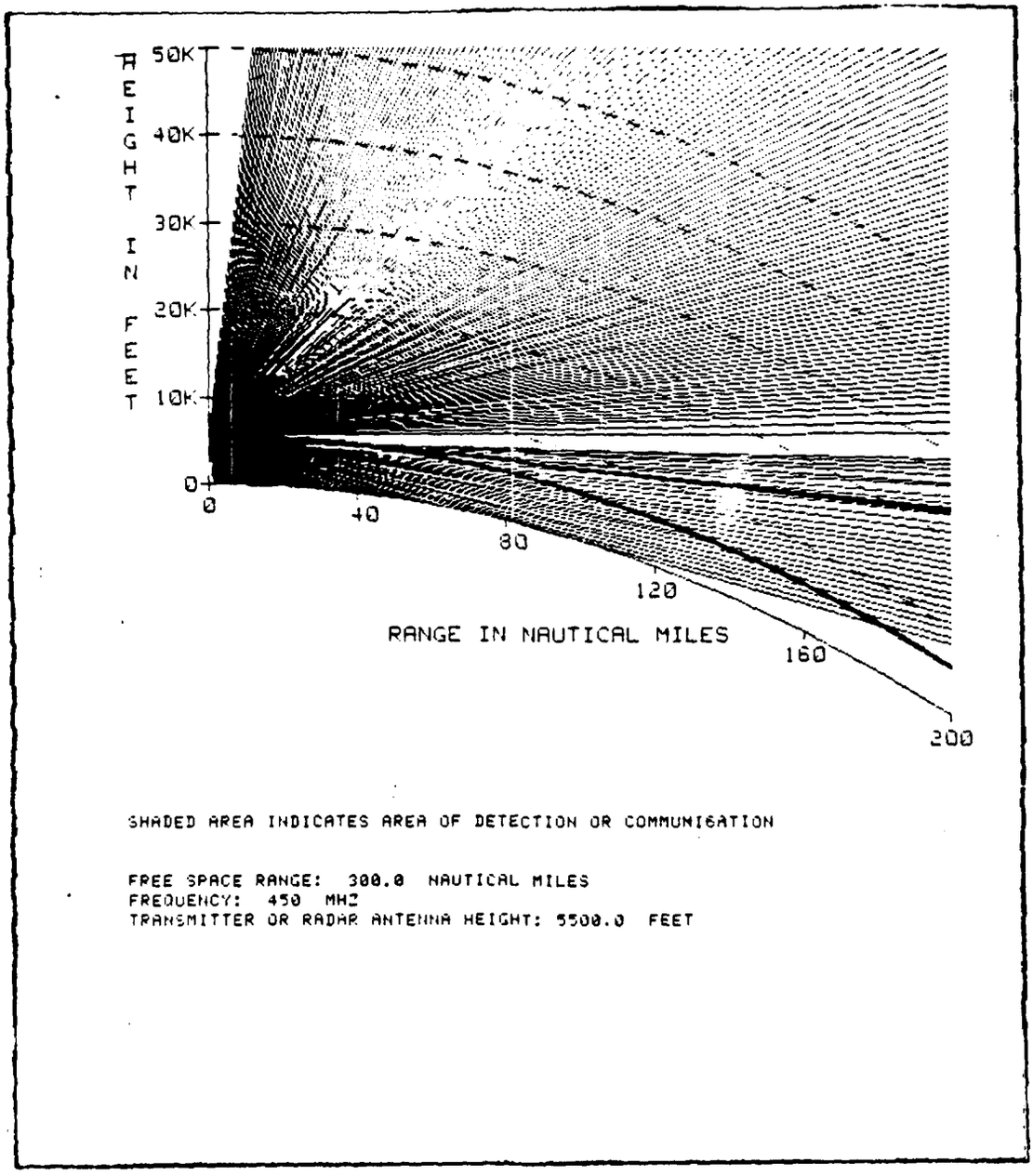

Figure C.9 Elev/Sub: -90/+60 N units/kft, 5.5 kft/5 kft. Radar Alt. 5,500 ft.

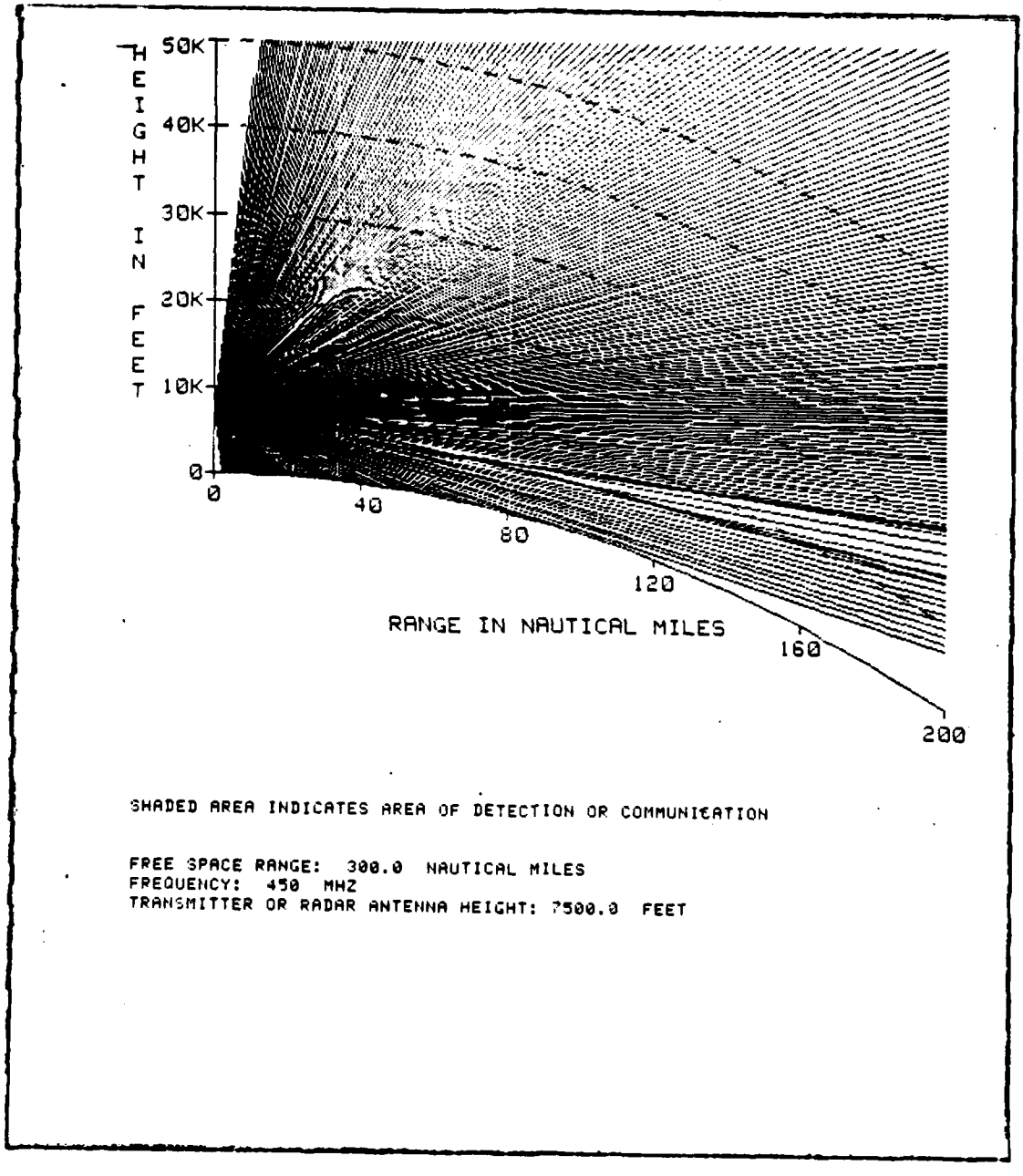

Figure C.10 Elev/Sub: -90/+60 N units/kft, 5.5 kft/5 kft. Radar Alt. 7,500 ft.

LIST OF REFERENCES

1. Hitney, H. V., et. al., IREPS Revision 2.0 Users Manual, Naval Ocean Systems Center Technical Document 481, September 1981.

2. Hall, M. P. M., Effects of the Troposphere in Radio Communications, Institute of Electrical Engineers, 1979.

3. Beach, J. B., "Atmospheric Effects on Radio Wave Propagation," Defense Electronics Technology, December 1979.

4. Bean, B. R. and Dutton, E. J., Radio Meteorology, National Bureau of Standards Monograph 92, March 1966.

5. Marcus, S., "A Model to Calculate EM Fields in Tropospheric Duct Environments at Frequencies Through SHF," IIT Research Institute, March 1982.

6. Naval Postgraduate School Report NPS-62-82-045 PR, A Simple Model for the Computation of Height Gain in the Presence of Elevated Tropospheric Ducts, by J. B. Knorr, p. 16, September 1982.

7. Skillman, J. L. and Woods, D. R., "Experimental Study of Elevated Ducts," Department of Defense, Fort Meade, Maryland, 1977.

8. Naval Science Department United States Naval Academy, Naval Operations Analysis, Naval Institute Press, 1974.

9. Lindsay, G. F., "Decisions and Principles of Choice," Class notes for course OA 4303, Naval Postgraduate School, 1984.

10. Larson, H. J., Introduction to Probability and Statistical Inference, John Wiley and Sons., 1982.

11. Skolnik, M. I., Introduction to Radar Systems, McGraw and Hill Book Co., Inc., 1962.

12. Davidson, K. L., "Meteorology Instruction Notes," Department of Meteorology, Naval Postgraduate School, 1985.

BIBLIOGRAPHY

Gossard, E. E., "Formation of Elevated Refractive Layers in the Oceanic Boundary Layer by Modification of Land Air Flowing Off Shore," NOAA/ERL/Wave Propagation Laboratory, August 1981.

Hillier, F. S. and Lieberman, G. J., Operations Research, Holden and Day Inc., 1967.

Hoaglin, D. C., Mosteller, F., and Tukey, J. W., Understanding Robust Exploratory Data Analysis, John Wiley and Sons Inc., 1983.

Hughes, W. P., Military Modeling, Military Operations Research Society, Inc., 1984.

Ko, H. W., Sari, J. W., and Skura, J. P., "Anomalous Microwave Propagation Through Atmospheric Ducts," John Hopkins University/Applied Physics Laboratory, November 1983.

Matthews, P. A., Radio Wave Propagation V.H.F. and Above, Chapman and Hall Ltd., 1965.

Raiffa, H., Decision Analysis, Addison and Wesley Publishing Co., July 1970.

Romano, A., Applied Statistics for Science and Industry, Allyn and Bacon, Inc., 1977.

Saxton, J. A., Radio-wave Propagation in the Troposphere, Elsevier Publishing Co., 1962.

INITIAL DISTRIBUTION LIST

		No. Copies
1.	Defense Technical Information Center Cameron Station Alexander, Virginia 22314	2
2.	Library, Code 0142 Naval Postgraduate School Monterey, California 93943	2
3.	W.J. Shaw, Code 63Sr Naval Postgraduate School Monterey, California 93943	1
4.	T.H. Hoivik, Code 55Ha Naval Postgraduate School Monterey, California 93943	1
5.	R.R. Read, Code 55Re Naval Postgraduate School Monterey, California 93943	1
6.	R.J. Taylor Naval Warfare Analysis Department John Hopkins University Applied Physics Laboratory John Hopkins Road Laurel, Md. 20707	1
7.	Lt. Doug Grau 1815 5th Ave. N. Denison, Ia. 51442	1

END

FILMED

8-85

DTIC